Chapter 4

Baseline Hydrologic Studies in the Lower Elwha River Prior to Dam Removal

By Christopher S. Magirl, Christopher A. Curran, Rich W. Sheibley, Jonathan A. Warrick, Jonathan A. Czuba, Christiana R. Czuba, Andrew S. Gendaszek, Patrick B. Shafroth, Jeffrey J. Duda, and James R. Foreman

Abstract

After the removal of two large, long-standing dams on the Elwha River, Washington, the additional load of sediment and wood is expected to affect the hydrology of the lower river, its estuary, and the alluvial aquifer underlying the surrounding flood plain. To better understand the surface-water and groundwater characteristics of the river and estuary before dam removal, several hydrologic data sets were collected and analyzed. An experiment using a dye tracer characterized transient storage, and it was determined that the low-flow channel of the lower Elwha River was relatively simple; 1–6 percent of the median travel time of dye was attributed to transient-storage processes. Water data from monitoring wells adjacent to the main-stem river indicated a strong hydraulic connectivity between stage in the river and groundwater levels in the flood plain. Analysis of temperature data from the monitoring wells showed that changes in the groundwater temperature responded weeks or months after water temperature changed in the river. A seepage investigation indicated that water from the river was moving into the aquifer (losing reach) between 1.7 and 2.8 kilometers from the river mouth. Surface-water measurements and temperature and salinity data collected throughout the estuary helped to characterize the magnitude and nature of water movement in and out of the estuary. Salinity and stage sensors positioned in the estuarine network showed a strong surface-water connection between the river and estuary waters east of the river. In contrast, there was a weaker connection between the river and estuarine water bodies west of the river.

Introduction

Removal of the Elwha and Glines Canyon Dams on the Elwha River on the Olympic Peninsula of northwest Washington is expected to affect aquatic ecology, sediment transport, and fluvial geomorphology along the river, estuary, and nearshore within the Strait of Juan de Fuca (see Duda and others, 2008; Kloehn and others, 2008; Warrick and others, 2009; Draut and others, 2011; Duda and others, 2011b, chapter 1, this report). Because the Elwha dams currently are operated in run-of-the-river mode, the underlying hydrologic regime in the river will change only slightly after dam removal (Duda and others, 2011b, chapter 1, this report). The fate of the 19 million m^3 of sediment entrapped behind both dams, however, is expected to have significant effects on sediment transport, sediment-size distribution, and river-bed elevation (Czuba and others, 2011, chapter 2, this report; Warrick and others, 2011a, chapter 3, this report), as well as the biological communities downstream of the reservoirs and in marine waters (Duda and others, 2011a, chapter 7, this report).

As a result of changes in areal extent and bed elevation within the river corridor, the dam-removal project also is expected to affect the underlying framework of water movement throughout the lower Elwha River and its estuary. For example, channel complexity (that is, the potential for water to follow multiple flow paths, including recirculation zones, down the river corridor) within the river will likely be affected as sedimentation and the addition of large woody debris from sources upstream of the former dam sites enhance channel-migration potential (Kloehn and others, 2008). Significant channel change occurred near the river mouth as a result of the December 2007 peak-flow event, with an estimated recurrence interval of 40 years (Draut and others, 2011). Changes in sediment-size distribution in the bed of the main-stem river also may alter hydraulic connectivity between the river and groundwater in the surrounding flood plain. In turn, groundwater levels in the lower Elwha River flood plain may rise as sedimentation in the main-stem river elevates the bed and associated water levels (Pacific Groundwater Group, 2005).

Water exchange and transport through the estuary complex also is expected to be affected. The movement of water through the lower Elwha River estuary is governed by channel morphology in the main-stem Elwha River, sedimentology of the underlying alluvium, ocean processes of tides and waves, and temperature- and solute-driven flows between freshwater and saltwater. Conceptually, the estuary is a transient storage facility that captures the outgoing flux of freshwater flowing from the river to the Strait of Juan de Fuca. The specific areas of water exchange, however, are temporally and spatially complex.

The Elwha River mouth and estuary form an important habitat for young salmonids and other fish and wildlife species (Shaffer and others, 2009; Duda and others, 2011a, chapter 7, this report), and adjacent terrestrial habitats support a diverse complex of wetland and riparian vegetation (Shafroth and others, 2011, chapter 8, this report). Within these water bodies, river water, groundwater, and seawater mix providing brackish conditions that change with tides, storms, and seasons. These water-level and salinity dynamics exert a strong influence over biotic communities in river mouth estuaries (Mitsch and Gosselink, 1993; Keddy, 2000; Shafroth and others, 2011, chapter 8, this report). Mixing of freshwater and saltwater offshore of the river mouth within the river plume is described more fully by Warrick and others (2011b), chapter 5, this report, and Warrick and Stevens (2011).

Previous Studies

Few studies have addressed the hydrology of the lower Elwha River. The Pacific Groundwater Group (2005) completed a groundwater model for the lower Elwha River flood plain to predict the response of groundwater elevations after a presumed 0.8-m post-dam-removal aggradation in the channel. The model was calibrated using groundwater data from wells distributed throughout the valley-wide flood plain. A strong hydraulic connection between river stage and the wells adjacent to the river channel was documented under low-flow and peak-flow conditions using groundwater data and model simulation results (Pacific Groundwater Group, 2005). The correlation in groundwater response to river stage decreased with distance from the main-stem river and was negligible along the coastline at the eastern boundary of the flood plain where tidal influences dominated groundwater elevations (Pacific Groundwater Group, 2005). The correlation in groundwater response to river stage decreased with distance from the main-stem river and was negligible along the coastline at the eastern boundary of the flood plain where tidal influences dominated groundwater elevations (Pacific Groundwater Group, 2005). Based on data from aquifer tests, Pacific Groundwater Group (2005) concluded that the hydraulic conductivity of the lower Elwha River aquifer was, on average, 220 meters per day (m/d), and ranged from 60 to 490 m/d.

Detailed velocity measurements were made at five transects near the river mouth (Curran and others, 2008). Similarly, recent monitoring of stream temperature noted an increase in mean annual stream temperature, and a decrease in diurnal temperature fluctuations, in the regulated reach downstream of Glines Canyon Dam compared with the unaltered upstream reach (Connolly and Brenkman, 2008).

This warming of stream temperature downstream of the dams was attributed to heat storage in the Lake Mills reservoir (Wunderlich and others, 1994). However, thermal data characterizing specific temperature distribution of free-flowing and quiescent water bodies located throughout the lower Elwha River corridor are rare.

Purpose and Scope

The U.S. Geological Survey (USGS), in collaboration with the Lower Elwha Klallam Tribe, the National Park Service, and other Federal and state agencies, has worked to characterize the hydrologic framework of the lower Elwha River. This chapter documents research and monitoring efforts that were completed before dam removal and have not been published elsewhere. Much of the data were collected with support from the USGS multi-disciplinary Coastal Habitats in Puget Sound (MD-CHIPS) initiative (Duda and others, 2011b, chapter 1, this report). The research, largely intended to establish baseline hydrologic data sets before dam removal, included efforts to (1) characterize transient storage in the lower river, (2) monitor flood-plain groundwater movement and hydraulic connection with the main-stem river as well as identify areas of exchange between surface water and groundwater, and (3) identify primary hydrologic fluxes and exchanges of groundwater and surface water of river and marine origin in the estuary complex (Duda and others, 2011b, chapter 1, this report). This estuary complex is biologically significant as a rearing habitat for some species of juvenile salmonids, especially Chinook salmon, which is on the Federal endangered species list (Duda and others, 2011a, chapter 7, this report).

Hydrologic Studies in the Lower Elwha River

Numerous measurements and data-monitoring efforts (table 4.1) were completed at several locations along the lower Elwha River flood plain (fig. 4.1) that enabled the characterization of key hydrologic aspects of the lower Elwha River. Transient storage in the river corridor was assessed using a dye tracer injected into the main stem during low flow. Groundwater movement was evaluated using water-elevation data from wells positioned throughout the wider valley flood plain. Surface-water/groundwater exchanges were identified using a seepage investigation (a technique used to identify river reaches that are gaining or losing surface-water flow to the aquifer; see, for example, Ely and others, 2008) and temperature data from the beds of surface-water bodies to identify regions of groundwater upwelling. Finally, a diverse assemblage of surface-water measurements, tidal data, thermal signatures, and specific conductance measurements were used to infer how water flows in and out of the estuary.

Due to its importance to aquatic habitat, considerable hydrologic analysis was focused on the estuary, which includes the network of surface-water bodies and interconnecting channels near the river mouth (fig. 4.2). The water bodies and channels east of the river mouth are collectively referred to as the east estuary. Following the naming convention established by Duda and others (2011b, chapter 1, this report), the east estuary consists of ES1, a water body closest to the river, ES2, a larger water body farther to the east that occupies a former river-mouth channel, and Bosco Creek, a spring-fed water source that originates in the flood plain east of the main-stem river, flows into the eastern edge of ES2, and is the only known fresh surface-water flow into the east estuary (fig. 4.2). The prominent channel that connects ES1 to the main stem Elwha River just upstream of the river mouth is referred to as the ES1 outlet channel. West of the river, two disconnected surface-water bodies comprise a smaller estuary assemblage. Just west of the river, a secondary distributary channel named the West Estuary Channel (WESC) (Duda and others, 2011b, chapter 1, this report) is, at times, hydraulically connected to the main-stem river. Farther west, beyond a flood-control levee is Dudley Pond, a water body disconnected from the main-stem river (fig. 4.2).

Transient Storage in the Lower Elwha River

Current methods of assessing in-stream habitat focus on physical measurements of specific habitat elements (for example, Fitzpatrick and others, 1998), but do not integrate across spatial scales or provide a direct measure of ecosystem function. Transient storage in a stream or river reach refers to any mechanism that slows down the bulk flow of water. Typically this results from in-channel features and exchange with shallow streambed sediments within the hyporheic zone (fig. 4.3). Therefore, there is a greater potential for transient storage in a stream that contains heterogeneous habitat elements at both large scales (for example, pool-riffle sequences and secondary channels) and small scales (heterogeneous substrate and in-channel vegetation).

Table 4.1. Surface-water and groundwater sampling sites along the lower Elwha River, Washington.

[**Abbreviations**: RKm, river kilometer; CT, conductivity and temperature sensors; CTD, conductivty and temperature sensors equipped with transducers to measure water depth; n/a, not applicable]

Decimal latitude	Decimal longitude	Site identifier	Data collection dates	Data collected
48.145808	-123.559370	TStn 1	8-1-09–12-18-09	Thermal
48.146438	-123.560386	TStn 2	8-1-09–12-21-09	Thermal
48.148155	-123.561795	TStn 3	8-1-09–12-11-09	Thermal
48.146982	-123.562848	TStn 4	8-2-09–8-8-09	Thermal
48.148670	-123.560036	TStn 5	8-2-09–8-8-09	Thermal
48.147375	-123.561944	TStn 6	8-2-09–8-8-09	Thermal
48.147515	-123.563160	ES1	7-28-07–3-29-10	CTD
48.147582	-123.561344	ES2	6-3-08–4-1-10	CT/CTD
48.145493	-123.567366	WESC	5-29-09–5-4-10	CT/CTD
48.144483	-123.568045	Dudley Pond	5-14-09–4-19-10	CTD
48.139917	-123.548006	AFN 256	11-9-07–8-27-09	Groundwater and thermal
48.135036	–123.554297	AFN 254	11-9-07–8-27-09	Groundwater and thermal
48.131425	–123.550747	MWGR	11-9-07–8-27-09	Groundwater and thermal
48.138014	-123.548883	AFN 259	11-9-07–8-27-09	Groundwater and thermal
48.147250	-123.563444	Acoustic Doppler velocity meter	6-3-08–9-2-08	Velocity/depth
48.145639	-123.563461	Estuary I/O flow	6-3-08–9-2-08	Discharge
48.144589	-123.556925	Bosco Creek	6-3-08–8-3-08	Discharge
48.119203	-123.553661	State hatchery outflow	9-24-07	Discharge
48.144314	-123.563133	RKm 0.4	9-24-07–9-26-07	Discharge
48.144111	-123.562589	RKm 0.4	9-24-07–9-26-07	Discharge
48.141756	-123.565631	RKm 0.8	9-25-07–9-26-07	Discharge
48.135597	-123.560611	RKm 1.7	9-25-07–9-26-07	Discharge
48.131853	-123.551247	RKm 2.2, old channel	9-26-07	Discharge
48.128217	-123.559203	RKm 2.6	9-24-07	Discharge
48.126889	-123.558706	RKm 2.8	9-24-07, 9-26-07	Discharge
48.121350	-123.554619	RKm 3.5	9-24-07	Discharge
48.118444	-123.554806	RKm 3.8	9-24-07	Discharge
48.114167	-123.553611	RKm 4.4	9-24-07–9-26-07	Discharge
48.142714	-123.563164	Tommy Boy	9-26-07	Discharge
48.120878	-123.555072	Trib 2	9-24-07	Discharge
48.129589	-123.554500	Trib 3	9-26-07	Discharge
48.131167	-123.551561	Trib 4	9-26-07	Discharge
48.136017	-123.558011	Trib 5	9-25-07–9-26-07	Discharge
48.137722	-123.559817	Trib 6	9-25-07–9-26-07	Discharge
48.143425	-123.562283	Tribal hatchery	9-26-07	Discharge
48.120171	-123.554580	Dye deployment	9-29-09	n/a
48.126030	-123.557110	Station 1	9-29-09	Dye concentration
48.131721	-123.557124	Station 2	9-29-09	Dye concentration
48.141685	-123.565316	Station 3	9-29-09	Dye concentration

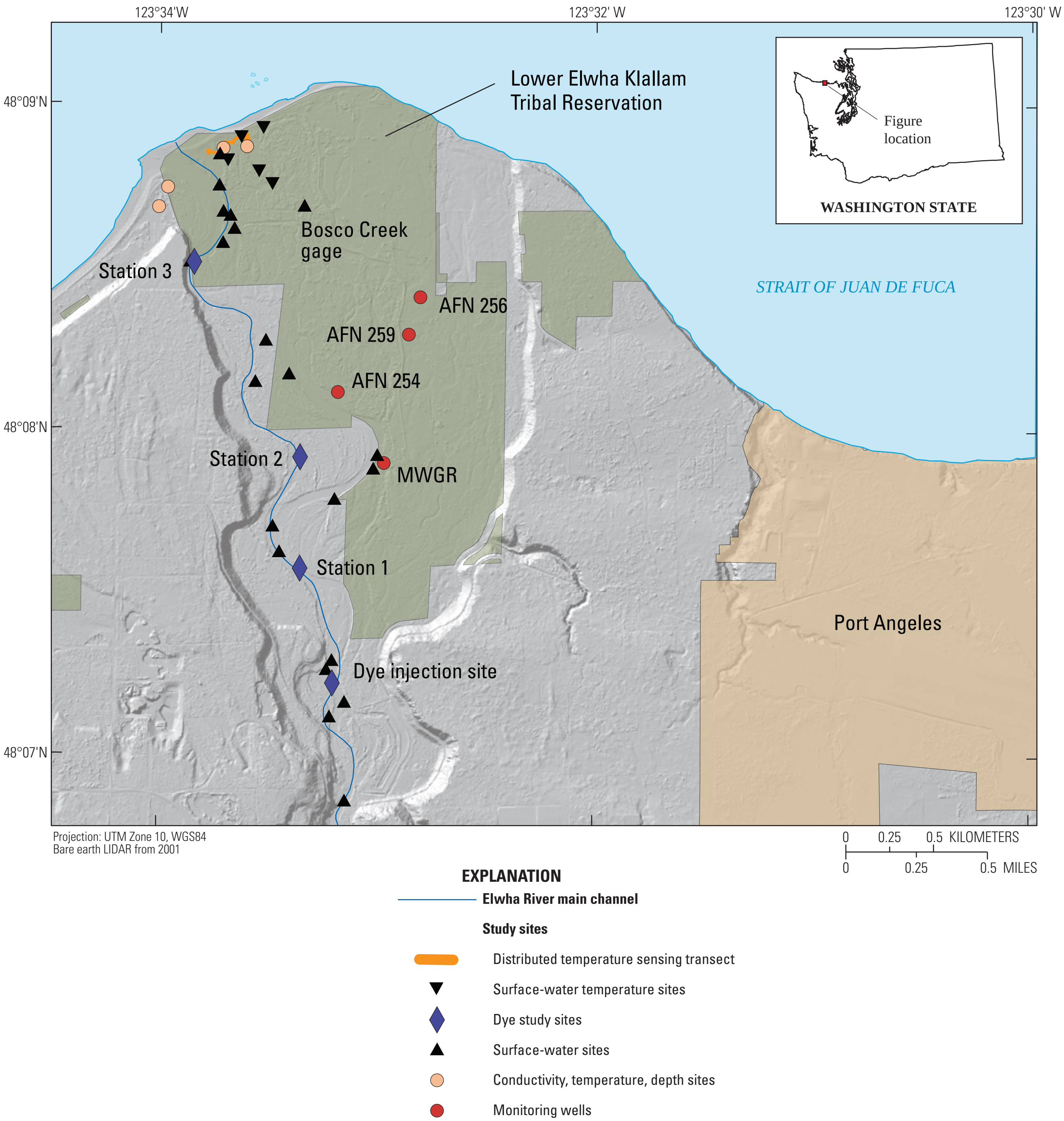

Figure 4.1. Locations of hydrologic monitoring sites, lower Elwha River and estuary, northwest Washington.

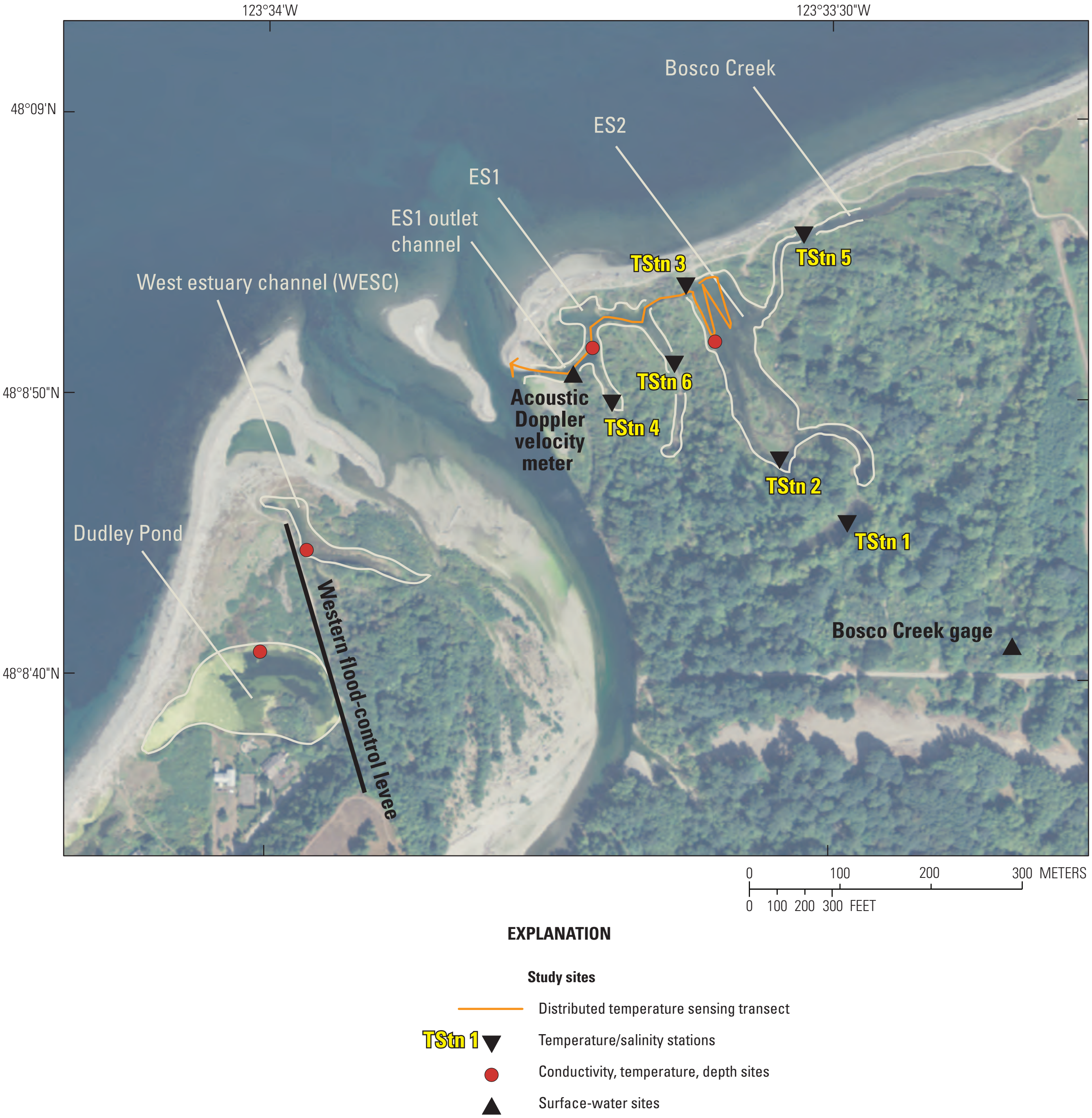

Figure 4.2. Locations of data collection sites near the Elwha River estuary, Washington.

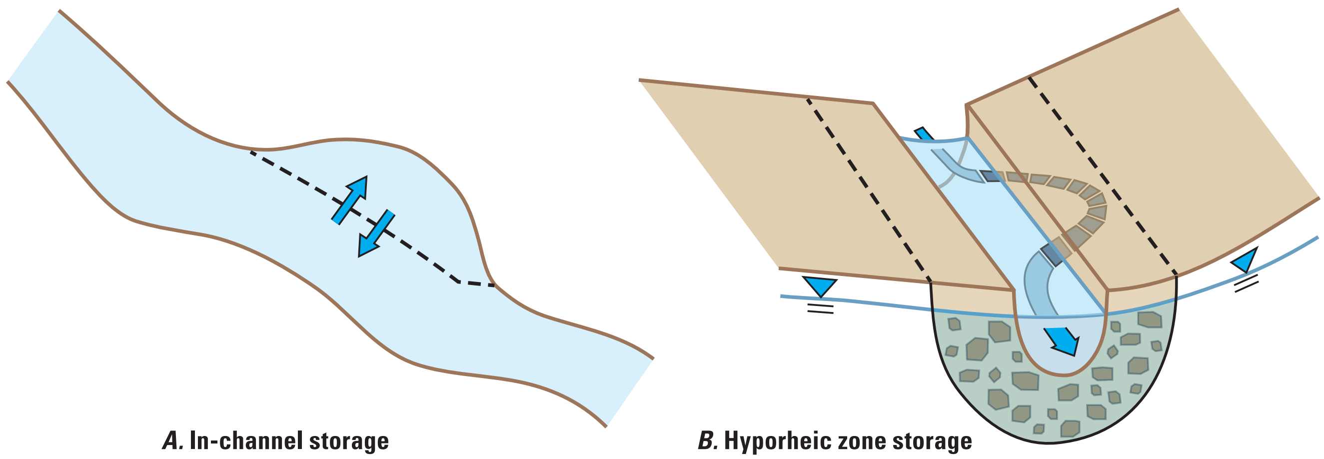

Figure 4.3. Conceptual diagram of transient storage, defined as the temporary retention of water due to (*A*) in-channel storage elements like pools and eddies, and (*B*) the hyporheic zone (shallow stream sediments). (Adapted from Runkel, 1998.)

Transient storage in streams has been shown to increase in the presence of large woody debris (Valett and others, 2002), in-stream vegetation (Harvey and others, 2003), channel meanders (Boano and others, 2006), and pool-riffle sequences (Gooseff and others, 2006), all of which contribute to the habitat needs of stream biota. Measures of transient storage in a reach, therefore, provide an indicator of habitat quality that is integrated across the spatial scales. Streams with high degrees of habitat heterogeneity (complexity) generally have a high potential to retain water in transient storage.

The amount of transient storage in a reach can be important for ecosystem functions of rivers and streams. For example, the longer that water remains in contact with stream sediment, the greater the opportunity for transformation and uptake of solutes in the reach becomes. Therefore, a complex channel with greater transient storage can lead to enhanced nutrient uptake (Valett and others, 1996; Butturini and Sabater, 1999; Bukaveckas, 2007) and increased stream metabolism (Mulholland and others, 1997). In the lower Elwha River, measurements of transient storage before and after dam removal will be an important tool for documenting changes in transient storage and its potential influence on solute uptake (for example, nutrients released from decaying salmon carcasses).

Reach-averaged transient storage commonly is measured by injecting a solute tracer into the stream and measuring the tracer concentrations downstream, yielding a solute breakthrough curve (fig. 4.4). If the tracer simply advects (that is, moves with the flow with little mixing or diffusion) through the reach because few habitat elements slow the main flow, the solute breakthrough curve will have a relatively high peak concentration and a quick return to background concentrations (fig. 4.4; solid line). Observation of a relatively lower peak concentration within the solute breakthrough curve and a slow return to background concentrations, indicates increased transient storage (fig. 4.4; dashed line). A solute-transport model that includes transient storage components to fit the field data from the tracer experiments can be used to quantitatively determine the amount of transient storage in a study reach. Previous work has shown that a complex channel structure (that is, multiple flow paths, pools, wood jams) increases the potential for transient storage, and that solute-injection experiments show promise for documenting this relation (Gooseff and others, 2007).

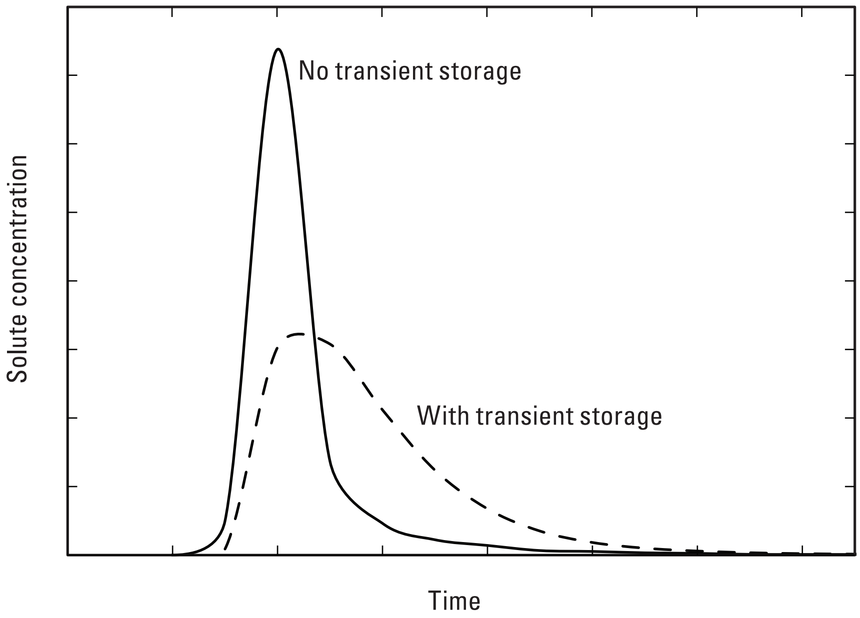

Figure 4.4. Theoretical downstream response to an instantaneous input of solute tracer. With little or no transient storage in the stream reach, the tracer is influenced only by advection and dispersion (solid line). A stream reach with significant transient storage will result in spreading of the peak with distance from the injection site (dashed line). (Adapted from Runkel, 1998.)

Transient storage was determined in the lower Elwha River using a dye-tracer experiment in which a slug of fluorescent dye was added to the main-stem river, while downstream detection instruments recorded dye concentration response over time. These temporal concentration data then were combined with a transient-storage model (Runkel, 1998) to assess overall transient storage for the study reach.

On September 29, 2009, a solute injection experiment using a non-toxic dye tracer, Rhodamine WT (RhWT), was completed on the lower Elwha River (fig. 4.1), timed to take advantage of autumnal low flow. The dye-injection site was in a section of the river with confined banks (about 3.9 km upstream of the river mouth), and the tracer was released into a riffle to enhance mixing (fig. 4.5). Another riffle farther downstream again mixed the dye throughout the width of the river. A total of 6.3 liters of 20 percent active ingredient Rhodamine WT was added to target a peak concentration of about 50 µg/L at the most downstream detection site, using the equations of Kilpatrick and Cobb (1985). To offset density differences and to improve lateral mixing, the tracer was added to the river simultaneously by three individuals spaced across the river at the injection site (fig. 4.5).

Concentration of dye was measured at three locations downstream of the injection site (fig. 4.1) using automated field fluorometers (SCUFA) that measured the fluorescence of the added tracer in the river with a reported detection limit of 0.04 µg/L (Turner Designs, Inc, 2004). Measurements of fluorescence were recorded at 1-minute intervals throughout the duration of the experiment to determine the solute breakthrough curves at each site. A SCUFA mount assembly for each instrument was secured to the riverbed using a cinderblock anchor attached to a float. The SCUFA then was affixed to this mount assembly so that the instrument was positioned at a point in the water column 0.75 m below the water surface. The three instruments were calibrated with simultaneous placement in the river for 10–15 minutes before and after the experiment to determine the bias in fluorescence readings between individual meters, and to assess potential instrument drift during the experiment.

Figure 4.5. Dye study in the lower Elwha River, Washington, September 29, 2009. (*A*) USGS hydrologist mixing the Rhodamine WT solution prior to slug injection; *(B*) three USGS hydrologists introducing the rhodamine into a riffle to enhance lateral mixing of the tracer; (*C*) dye tracer just downstream of the injection riffle, where the plume is spreading longitudinally and laterally in the slow moving water before reaching the next downstream riffle; and (*D*) looking downstream as the dye tracer approaches the first monitoring station. Main channel storage is evident on the left side of the channel in a slower moving backwater area, shown by the arrow. (Photographs taken by (*A*) James R. Foreman, U.S. Geological Survey and (*B, C, D*) Christopher A. Curran, U.S. Geological Survey.)

The three SCUFAs, referred to as Station 1, Station 2, and Station 3 (table 4.1), were placed 0.7, 1.5, and 3.0 km downstream of the injection site, respectively (fig. 4.1). River discharge was measured at Stations 1 and 2 during the experiment using a hand-held acoustic Doppler velocimeter, and at Station 3 using an acoustic Doppler current profiler mounted on a tethered boat. The theory of operation of these hydroacoustic technologies is well documented (see, for example, Yorke and Oberg, 2002). Standard USGS measurement protocols were followed for both methods, and measurement error was assumed to be less than 5 percent (Mueller and Wagner, 2009; Turnipseed and Sauer, 2010).

Rhodamine travel times to each SCUFA monitoring station were determined by plotting the tracer response at each SCUFA station compared to time (fig. 4.6), and the time when peak concentration was reached represented the average travel time to that monitoring station from the injection site (Kilpatrick and Wilson, 1989). Average travel times to each station from the injection point were 0.42, 0.93 and 1.57 hours, respectively. Measured river discharge was 9.46 m^3/s (334 ft^3/s) at Station 1, decreasing to 8.86 m^3/s (313 ft^3/s) at Station 2, and increasing to 9.85 m^3/s (348 ft^3/s) at Station 3 (table 4.2). For comparison, the daily discharge for that day as measured at USGS streamflow-gaging station 12045500 (Elwha River at McDonald Bridge near Port Angeles, Wash.) was 10.1 m^3/s (355 ft^3/s).

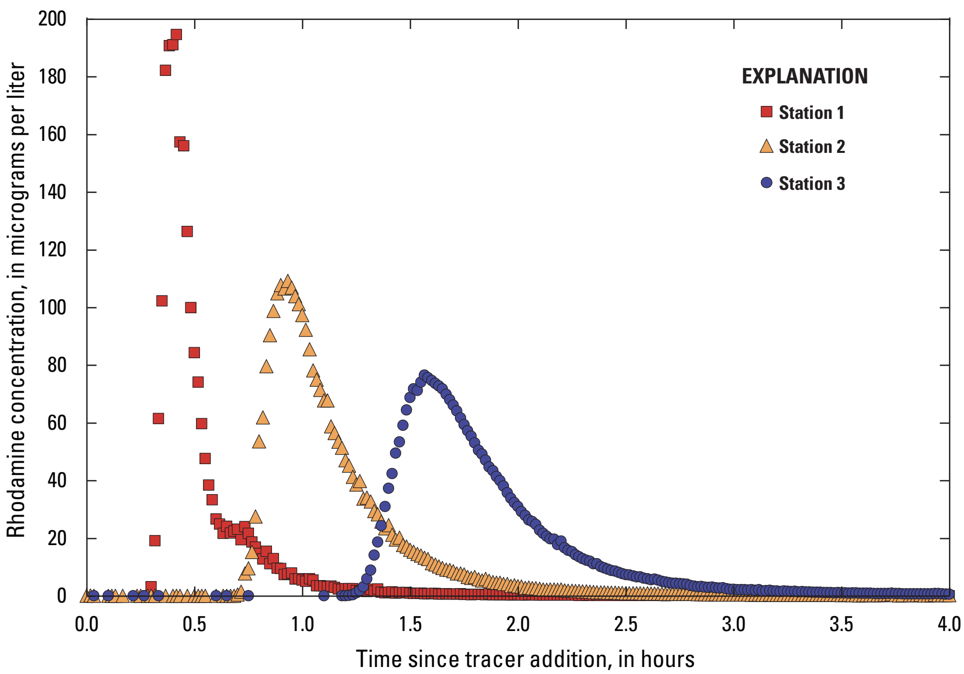

Figure 4.6. Measured rhodamine concentrations at monitoring stations 1, 2 and 3 after a slug injection of 6.3 liters of Rhodamine dye tracer in the lower Elwha River, Washington, September 29, 2009.

Table 4.2. Flow and cross section characteristics from manual discharge measurements, Elwha River, Washington, September 29, 2009.

[**Abbreviations**: m^3/s, cubic meter per second; m, meter; m^2, square meter; m/s, meter per second]

Station No.	Discharge (m^3/s)	Width (m)	Mean depth (m)	Area (m^2)	Velocity (m/s)
Station 1	9.46	46	0.58	26.8	0.37
Station 2	8.86	26	.43	11.5	.76
Station 3	9.85	33	.46	14.9	.67

Tracer breakthrough curves were simulated using the one-dimensional transport with inflow and storage (OTIS) model (Runkel, 1998) to estimate the amount of transient storage in the experimental reach. OTIS solves two differential equations developed by Bencala and Walters (1983) to calculate solute concentrations over time in the main channel and the storage zone of the stream reach. The changes in the river discharge measured through the study reach, presumably from water exchanges with the underlying aquifer, were incorporated into the modeling results. The model simulation results produced estimates of four hydrologic parameters used to calculate transient storage metrics. These output parameters (shown conceptually in fig. 4.7) include the dispersion coefficient for the reach (D), the main channel cross sectional area (A), storage zone area (A_s), and rate of exchange between the main channel and storage zone (α). From these parameter estimates, the metrics of transient storage can be determined, including the relative storage zone capacity (A_s/A) and the fraction of median travel time due to transient storage normalized against a 200-m long reach (F_{med}^{200}) which allows for future comparison with data from other rivers (Runkel, 2002). Discharge fundamentally alters solute transport within a stream; therefore, tracer studies ideally should be over a range of discharge. However, F_{med}^{200} has been shown to be a robust metric for assessing differences in transient storage across sites and through time (Runkel, 2002) and can be used as a primary indicator for tracking changes following dam removal. By calibrating this model for the study reach, metrics of transient storage are derived that serve as indicators of habitat complexity prior to dam removal.

To run the OTIS model, the tracer breakthrough curve at Station 1 was entered as the upstream model boundary condition. This input then was used to simulate the data at Station 2 and Station 3 through a non-linear least squares algorithm using the OTIS-P model (Runkel, 1998). OTIS-P uses the same numerical model as OTIS, but includes a parameter estimation subroutine to automatically fit the model to downstream tracer data by optimizing values for D, A, A_s.

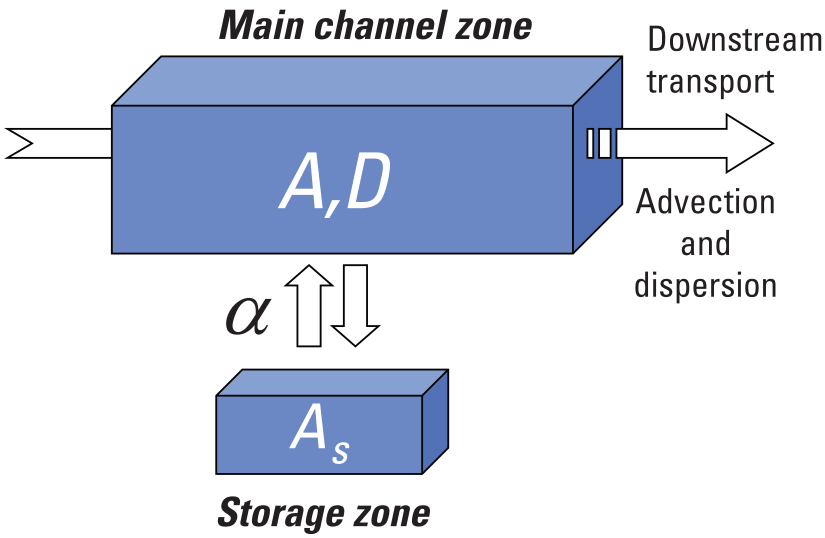

Figure 4.7 Conceptual diagram of one-dimensional transport with inflow and storage (OTIS) model showing advection and dispersion of solute (dye) within the main channel and exchange of solute into the storage zone. Four major model parameters are optimized to fit the calibration data including main-channel area (A), dispersion coefficient (D), storage zone area (A_s), and the exchange rate into the storage zone (α). (Adapted from Runkel, 1998.)

OTIS-P was executed for two model scenarios. The first scenario modeled the experimental reach as a single reach, with the Station 1 data used as the upstream boundary condition to simulate the response at Station 3. After the dams are removed, the entire reach between Stations 1 and 3 might remain intact as a single channel; therefore, this simulation will represent a baseline condition of the lower river before dam removal. The second scenario breaks up the experimental reach into two separate subreaches from (1) Station 1 to Station 2, and (2) Station 2 to Station 3, allowing transient storage properties to be assessed in each subreach. This sampling and modeling strategy provides some flexibility in the transient-storage analysis, and allows future studies to use the data collected even if the lower river channel experiences dramatic morphologic changes.

Transient storage model simulation results from OTIS-P simulations generally matched the measured Rhodamine curves for the single-reach scenario (fig. 4.8*A*), and the two-reach scenario (fig. 4.8*B*). Optimized parameters of transient storage from each model run indicate that little transient storage was in each reach (table 4.3). This observation is best illustrated by the values for F_{med}^{200}, the fraction of median travel time due to storage. In the single-reach scenario, F_{med}^{200} between Station 1 and 3 was 0.01, suggesting that approximately 1 percent of the travel time can be attributed to storage processes in the reach. For the two-reach scenario, F_{med}^{200} was higher in the first reach (0.06) when compared to the second reach (0.01). The relative size of the storage zone for the single-reach scenario, given by A_s/A, was 0.128, and for the two-reach scenario A_s/A was 0.237 and 0.160 for the upper and lower reaches, respectively. These A_s/A values indicate that the channel cross-sectional areas are larger than the theoretical storage-zone areas.

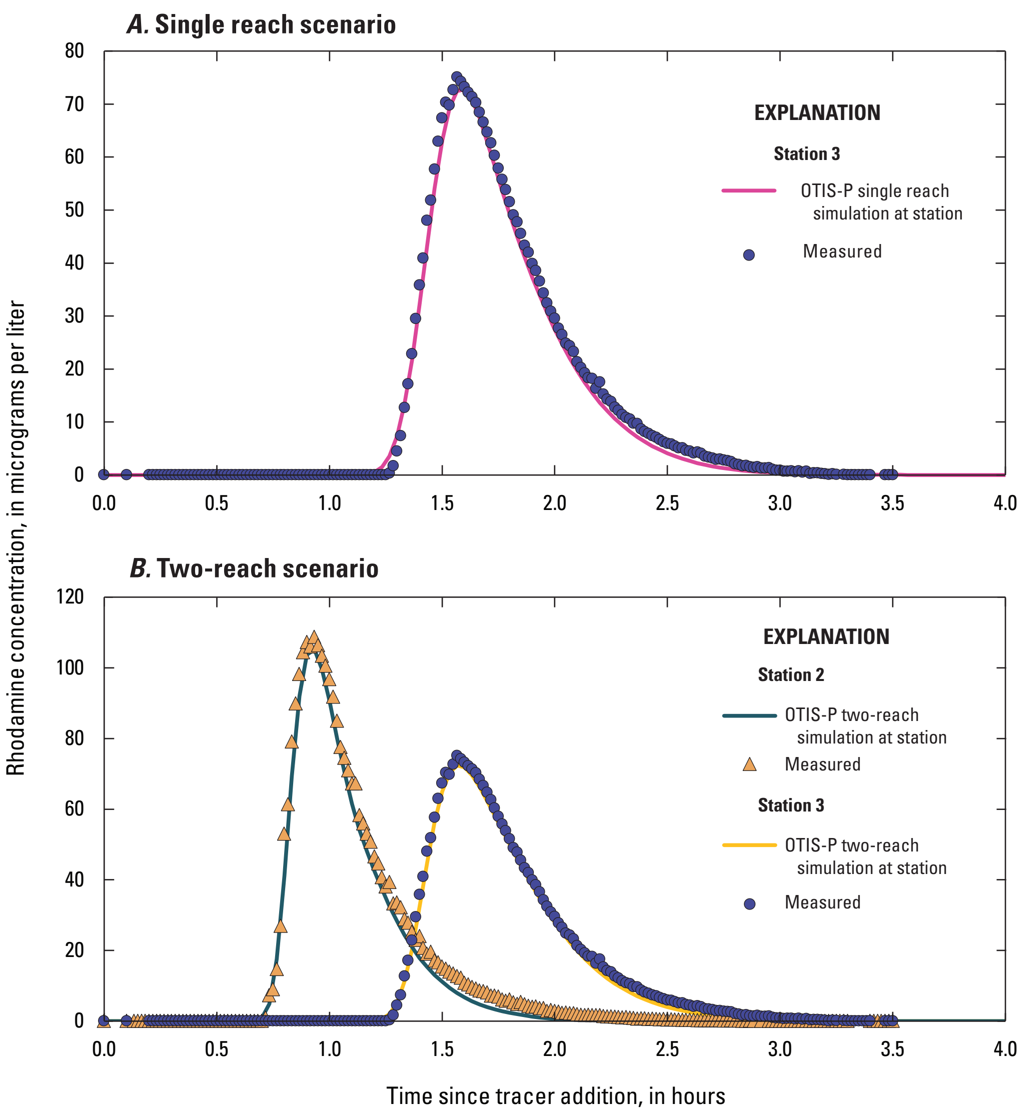

Figure 4.8 Measured and one-dimensional transport with inflow and storage (OTIS-P) simulated rhodamine breakthrough curves at (*A*) Station 3 for the single-reach scenario and at (*B*) Stations 2 and 3 for the two-reach scenario for the lower Elwha River, Washington.

Table 4.3. Optimized parameter estimates for the transient storage model using one-dimensional transport with inflow and storage (OTIS-P) and selected transient storage zone metrics, Elwha River, Washington.

[**Abbreviations**: D, dispersion coefficient; A, main channel cross-sectional area; A_s, storage zone cross-sectional area; α, storage zone exchange coefficient; A_s/A, relative storage-zone capacity; DaI, Damköhler number; F_{med}^{200}, fraction of median travel time due to storage normalized against a 200-meter long reach; m/s², meter per second squared; sec⁻¹; per second]

Reach	D (m/s²)	A (m²)	A_s (m²)	α (sec⁻¹)	A_s/A	F_{med}^{200}	DaI
Station 1 to 3	6.9	15.9	2.0	2.50E-04	0.128	0.01	8.9
Station 1 to 2	1.6	20.3	4.8	8.43E-04	.237	.06	7.2
Station 2 to 3	6.4	12.6	2.0	3.00E-04	.160	.01	4.7

To check how well the model simulated observed response in the river, the experimental Damköhler number (DaI) from each simulation was calculated. The DaI is a measure of how well the tracer experiment describes the transient storage processes of the experiment and is calculated by

$$DaI = \alpha \frac{(1 + A / A_s)L}{u}, \qquad (1)$$

where L is the reach length (Wagner and Harvey, 1997). Values of DaI close to 1.0 are ideal, but values between 0.1 and 10.0 indicate that the tracer experiment adequately describes the transient storage processes of the experiment (Wagner and Harvey, 1997; Harvey and Wagner, 2000). The DaI results for this study were all greater than 1.0 (4.7 to 8.9, table 4.3), but were within this optimal range. Thus, the values of DaI, and the quality of the visual fit to field data, indicate that the modeling approach was reasonable for this experiment.

The amount of transient storage in the experimental reach is small, likely due to high water velocity and a relatively simple channel (table 4.2). Generally, from 1 to 6 percent of the median travel time in the lower reach can be attributed to transient storage processes. With a change in sediment supply and large woody debris after dam removal, sedimentation and channel reorganization in the lower Elwha River are expected to increase channel-structure complexity. These changes are expected to translate into measurable increases in travel times.

Groundwater and Surface-Water Interactions

Water levels and temperatures were collected from 2007 to 2009 using self-contained data recorders in four monitoring wells positioned throughout the Elwha River flood plain. These groundwater data, coupled with streamflow and thermal patterns measured in the main-stem river, allowed for the analysis of the relative connectivity of the aquifer to the river. A seepage investigation in September 2007 included near simultaneous discharge measurements at multiple locations along the river channel to determine the volumetric exchange of surface water and groundwater. Finally, to better quantify the spatial distribution of groundwater flow feeding into the east estuary, thermal patterns of the estuary bed were measured over a 20-hour period in September 2008.

Water Level Measurements near the Lower Elwha River

Four data recorders with vented pressure transducers were placed in established monitoring wells (fig. 4.1; table 4.1) to collect water level and temperature data from November 9, 2007, to August 27, 2009, at 1-hour intervals. Raw water-level data were adjusted to elevation in meters above sea level (NAVD 88) based on well-head elevation surveys by the Pacific Groundwater Group (2005). The two southern-most monitoring wells were on the river side of the eastern flood-control levee (Warrick and others, 2011a, chapter 3, this report) along the outer bend of a distributary channel that conveys overflow with increasing discharge. The farthest upstream of these two wells (MWGR; fig. 4.1) was about 2.7 km upstream of the river mouth, and the other well (AFN 254) was about 2.1 km upstream of river mouth. Of the other two monitoring wells, AFN 259 (fig. 4.1) was farther south and closer to the river, and AFN 256 was farther north and closer to the coastline.

Data collected at the four monitoring wells indicated a strong correlation between groundwater elevation and river stage throughout the year, regardless of the river discharge or the season (fig. 4.9). Data from AFN 259 and AFN 256, the two wells closest to the coastline, between June and September of 2008, demonstrated the strong coupling between groundwater elevation in the flood plain and stage in the river (fig. 4.10). Additionally, tidal influences also were apparent in these flood plain wells, although tidal influence seemed to be considerably smaller than the river influence. The response time between the peak river stage and the peak groundwater elevation ranged from hours to a few days. Continuous groundwater-elevation data collected from intermittent records from October 2002 through January 2005 showed similar characteristics (Pacific Groundwater Group, 2005).

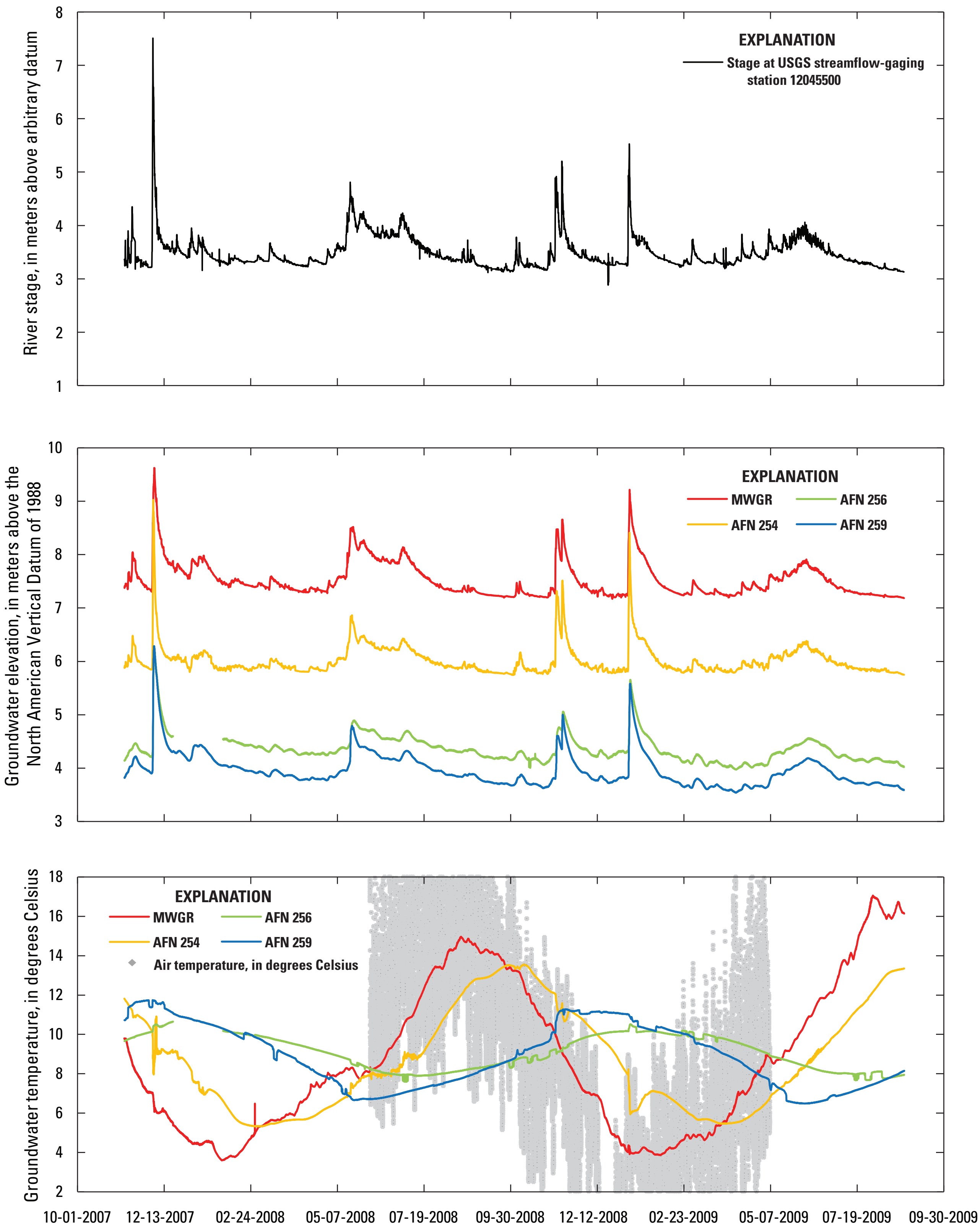

Figure 4.9 Groundwater elevations and temperatures from four monitoring wells in the Elwha River flood plain, in relation to river stage at U.S. Geological Survey streamflow-gaging station 12045500, Elwha River near Port Angeles, Washington, and air temperature at the Bosco Creek gaging station (12046523).

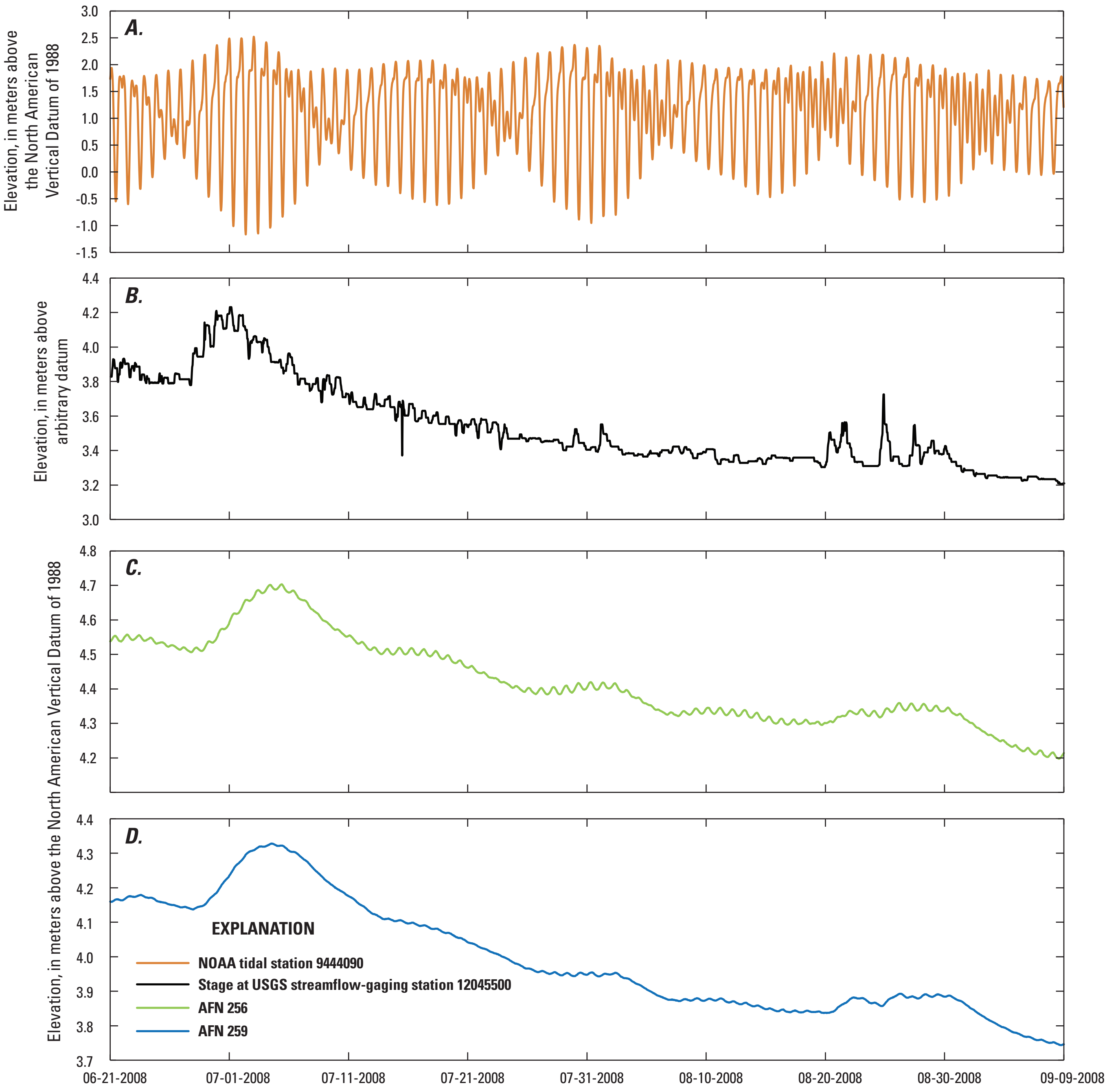

Figure 4.10. Water elevations representing (*A*) tidal stage at National Oceanic and Atmospheric Administration (NOAA) tidal station 9444090 in Port Angeles, Washington; (*B*) river stage measured at U.S. Geological Survey streamflow-gaging station 12045500, Elwha River near Port Angeles, Washington; (*C*) groundwater elevation in monitoring well AFN 256; and (*D*) groundwater elevation in monitoring well AFN 259. The data show the rapid response in groundwater elevation to changes in river stage. Both monitoring wells are at least 0.5 kilometers from the main-stem river and at least 1.0 kilometers from the coast.

Temperature data from the monitoring wells indicated that in contrast to the strong hydraulic connection of existed between the river and the aquifer, a relatively weak thermal connection existed between wells and, presumably, the main-stem river. Although daily water-temperatures measured directly in the lower Elwha River were not available, it was assumed that river temperature tracked air temperature, and air-temperature data were collected at 15-minute intervals with the BaroTROLL collector at USGS streamflow-gaging station 12046523, Bosco Creek near Port Angeles, Washington. These air-temperature data correlated well with the general trends in water temperature measured at MWGR (fig. 4.9). This new monitoring well is adjacent to the river channel and positioned 10–30 m from the distributary channel and likely is active for moderately large discharges. It seems likely that the delay or lag time between the temperature of water in MWGR and the river probably is on the order of a few days or weeks. At well AFN 254, about 100 m from the distributary channel, the warmest groundwater seems to occur about 1 month after the maximum air temperature (fig. 4.9). The occurrence of the warmest water at the flood-plain wells (AFN 259 and AFN 256) occurs 5–7 months after the maximum seasonal air temperatures (fig. 4.9).

Seepage Investigation in the Lower Elwha River

A seepage investigation from September 24 – 26, 2007, determined stream-flow gains and losses in the lower 4.4 km of the Elwha River. This investigation consisted of 18 discharge measurements collected at 8 sites on the main stem, and 4 sites on tributaries along the river (U.S. Geological Survey, 2007). Standard methods were followed for measuring discharge using a current meter for 8 measurements, an acoustic Doppler velocimeter for 6 measurements, and an acoustic Doppler current profiler for 4 measurements (Mueller and Wagner, 2009; Turnipseed and Sauer, 2010). For the seepage investigation, all discharge measurements were assumed to have an accuracy of 5 percent. Discharge measurements were made during autumn low flow to capture base-flow conditions when surface-water/groundwater interactions are most apparent.

During the 3-day seepage investigation, discharge at USGS streamflow-gaging station 12045500, the Elwha River at McDonald Bridge near Port Angeles, Washington, was constant at 10.25 m^3/s on September 24, 2007, and increased to 11.47 m^3/s on September 25, 2007, and remained constant for the rest of the seepage investigation (fig. 4.11). To allow direct comparison of discharge data between days, discharge measurements made on September 24, 2007, were adjusted upward by 1.22 m^3/s (the difference between background discharge of 11.47 m^3/s and 10.25 m^3/s) using the McDonald Bridge discharge values. Additionally, discharge measurements were adjusted for tributary inflow by subtracting all upstream tributary inflows from the main-stem Elwha River discharge measurements.

Elwha River discharge measurements that have been adjusted for variations in the hydrograph and tributary inflows show synoptic downstream variations in the flow that may be attributed to groundwater/surface-water exchange, tidal fluctuations in the estuary, measurement error, or some other factors (fig. 4.12). The variations in the discharge data at the section of river between 4.4 and 2.8 km upstream of the river mouth are within the uncertainty of the individual measurements; however, there may be a slight groundwater/surface-water exchange. Discharge measurements collected on the same day in the main-stem river between 2.8 and 1.7 km upstream of the river mouth indicated that about 10 percent of the Elwha River discharge seeped into the groundwater system. Discharge data downstream of 1.7 km from the river mouth indicated strong gains to the Elwha River on September 25, and no change on September 26 (fig. 4.12). However, the flow measurements on September 25 were made when the tide was falling, whereas the flow measurements on September 26 were made just after low tide. The differences in the adjusted flows near the river mouth between these 2 days likely were caused by the changing flow conditions in the estuary as water was stored and released to the river. Based on uncertainty of measurements, there were no clear trends indicating groundwater losses or gains in the lower 1.7 km of river or in the section of river upstream of a point 2.8 km from the river mouth.

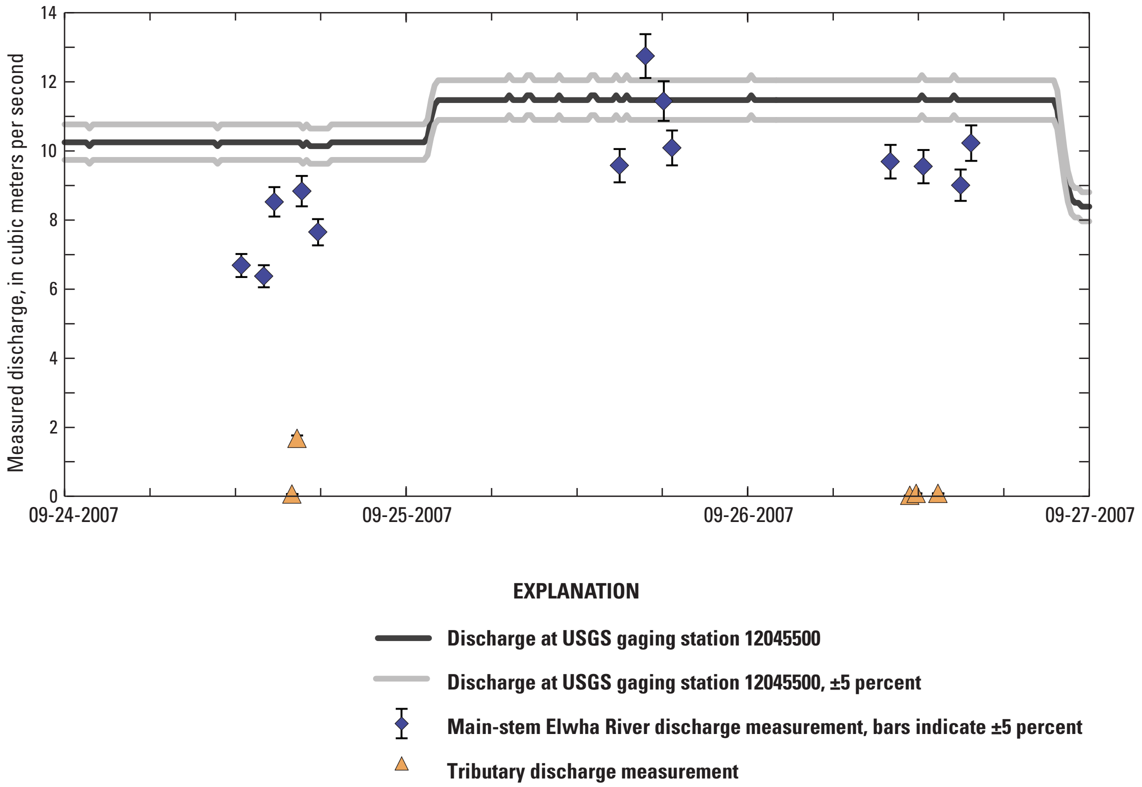

Figure 4.11. Discharges measured during the 3-day seepage investigation in September 2007, on the lower Elwha River in relation to the discharge at U.S. Geological Survey (USGS) streamflow-gaging station 12045500, Elwha River at McDonald Bridge near Port Angeles, Washington.

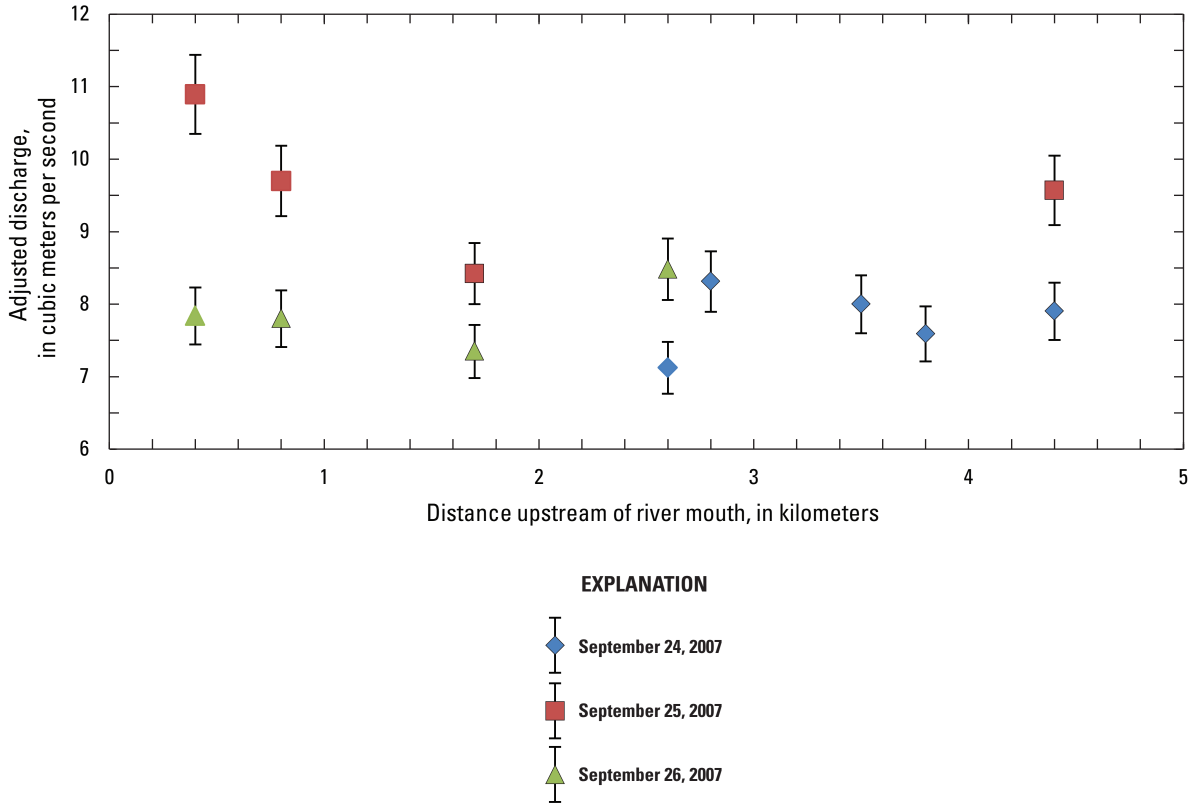

Figure 4.12. Adjusted synoptic discharge measurements in the lower Elwha River, Washington, for the September 2007 seepage investigation. Bars indicate ±5 percent.

Distributed Temperature Sensing in the Estuary

A water-temperature survey using fiber-optic distributed temperature sensing (DTS) technology (Selker and others, 2006; Tyler and others, 2009) was conducted in the east estuary in September 2008. The sampling sites covered much of the surface of the riverbed of the east estuary and ended in the main-stem river just upstream of the river mouth (fig. 4.2). The purpose of the temperature survey was to locate thermal signals (dampened diurnal fluctuations of surface-water temperatures) that could be attributed to groundwater discharge into the surface-water body. Water temperature also was used as a tracer to observe the circulation pattern of tidally induced mixing in the east estuary.

A field-portable Sensortran DTS unit was used with a 3-mm diameter steel and Kevlar reinforced single-ended fiber-optic cable dispensed from a portable reel containing about 1,500 m of cable. Temperature was recorded every 5 minutes at 1-m resolution along the cable length. The cable was calibrated on site with an ice bath at the DTS unit location. Using this arrangement, some degradation of precision occurs with distance from the DTS unit; however, DTS temperatures correlated well with Tidbit point sensors placed at multiple locations along the cable for comparison. Although 0.01 °C measurement precision has been demonstrated using similar DTS instruments (Selker and others, 2006), accuracy of measurements in both deployments were estimated to be 0.1 °C.

At the estuary site, DTS cable (900 m) was placed in the east estuary. The cable was laid over much of the bed of ES2, extended through connecting channels into ES1, extended farther through the ES1 outlet channel, and ended in the main-stem river just upstream of the river mouth (fig. 4.2). Turning points, used to guide the cable through the estuary complex without damage, were constructed of 2.5-cm steel pipe pounded into the substrate with a larger plastic-pipe sheath to protect the cable during placement. In most locations, the cable was placed on or near the bed substrate; an exception was in ES2 where thick algal mats and water depths often exceeding 1.2 m prevented the cable from resting directly on the bed. The estuary DTS cable was deployed over a 20-hour period and collected approximately 216,000 temperature measurements.

The weather during the DTS survey in the east estuary, on September 1–2, 2008, was warm and clear, with sun and little wind. Figure 4.13 shows the distribution of temperature along the DTS cable at transition times during the tidal cycle, when water flux into the estuary was changing. At 1400 on September 1, the water temperature in ES2 was a relatively warm 15 °C, but cold water of about 9 °C from the river was moving through the connecting channels into ES1 (fig. 4.13*A*). By 1700, at exactly high tide, cold water had ceased entering the connecting channel and nearly the entire cable was a relatively warm 16 °C (fig. 4.13*B*). This heating was caused by strong solar heating on September 1, 2008. By 2200, overall water temperature had decreased along the cable to about 14 °C in the ES1 and the ES1 outlet channels (fig. 4.13*C*). During the night and early morning, temperature generally dropped steadily in the smaller ES1 water body and connecting channels. Within ES2, however, the large thermal mass of the water body kept the water at about 15 °C throughout the night. Recorded temperature in ES2 also likely reflected the situation that algal mats suspended the DTS cable above the bottom of the water body. As a result, the temperature data collected in ES2 were from a depth location above the actual bed of the water body. Water temperature in the main-stem river fluctuated between 9 and 12 °C during the late afternoon and night, as warmer river water flowed over the top of the cooler marine water. Because the cable was laid on the bottom of Elwha River channel, cycles in the tide dictated whether relatively warm freshwater, or cool marine water, influenced thermal data in this location. By 1000 on September 2, as the tide approached its low point, solar heating had warmed most of the water in ES1 and ES2 (fig. 4.13*F*).

To analyze where the groundwater may have entered the estuary, the total variance of recorded temperature data over the 20-hour experiment is shown as a function of position along the cable (fig. 4.14). Due to the large thermal mass, and because the cable was suspended by an algal mat, overall thermal variance in ES2 was less than 2 °C. Nonetheless, assuming groundwater was cooler than 15 °C, no areas of groundwater influx to ES2 were identified with the experiment. Variance also was small between 180 and 200 m at a section of cable in the middle of ES1 (fig. 4.14). During the course of the experiment, temperature at this location in the cable ranged between about 13 and 14 °C, which is small compared to sections of the cable placed elsewhere where temperature fluctuated as much as 5 °C. The area of low variance is the short yellow section of cable in ES1 surrounded by red at 1700 on September 1 (fig. 4.13*B*), or the same yellow section of cable surrounded by cyan at 0700 on September 2 (fig. 4.13*E*). This small variance was interpreted to be a region of strong groundwater upwelling, probably associated with a relict fluvial channel of coarse sediment and relatively large hydraulic conductivity. Two other regions of decreased thermal variance were apparent near 155 and 76 m (fig. 4.14), also suggesting groundwater influx though the strength of the signal was smaller than in the region from 180 to 200 m.

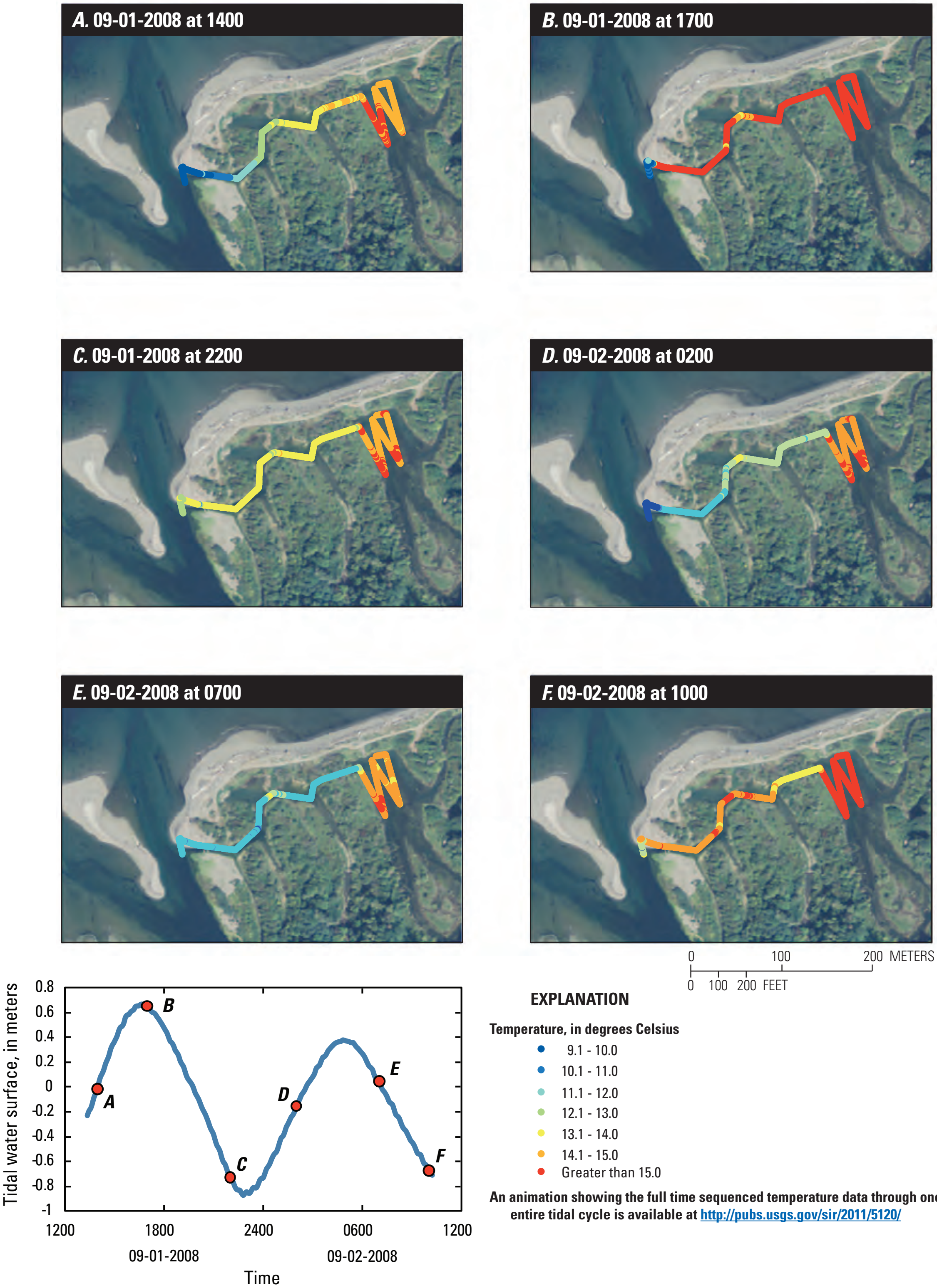

Figure 4.13. Photographs and graph showing temperature along a distributed temperature sensor (DTS) array positioned along the riverbed in the east estuary of the Elwha River between 1400 on September 1, 2008, and 1000 on September 2, 2008. Tidal stage at the National Oceanic and Atmospheric Administration tidal station 9444090 in Port Angeles, Washington, shows the influence of tides on surface-water exchange with the estuary.

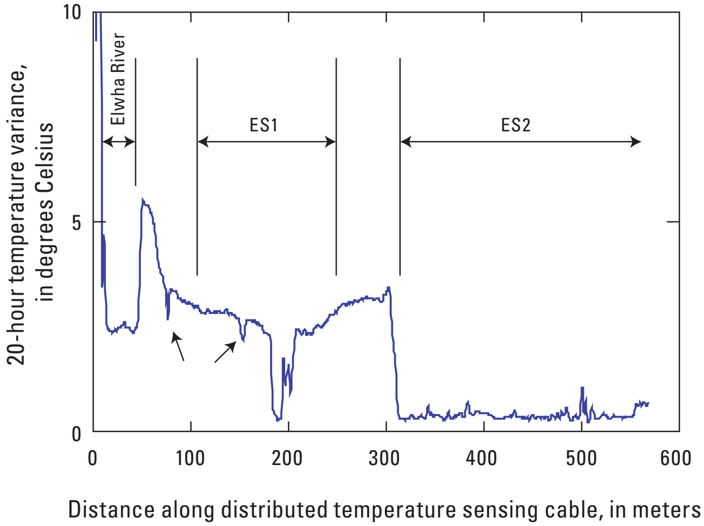

Figure 4.14. Variance in temperature fluctuation along the distributed temperature sensor array along the bed of the east estuary for the 20-hour period of data collection, Elwha River, Washington, September 1–2, 2008. Locations at 25 to 45 meters were in a section of the cable in the main stem of the Elwha River. Locations 320 meters and greater were sections of the cable in the ES2 water body. A prominent area of relatively small temperature variation from 180 to 200 meters likely was caused by strong groundwater upwelling. Similar reduced variation near 155 and 76 meters (indicated by arrows) might also reflect groundwater upwelling although the strength of upwelling was less pronounced than in the interval from 180 to 200 meters.

Water Data Collected within the Estuary

Qualitative observations of surface-water dynamics in the Elwha River estuary show the strong influence of tidal patterns and river flow dynamics (fig. 4.15), but do not explain the role of groundwater interactions, or quantify the relative contributions of water sources flowing to, and from, the estuary. By collecting temperature, salinity, stage, and surface-water velocity data at strategic locations in the estuary system, in addition to tidal information for the Strait of Juan de Fuca, a greater understanding of water movement through the complex was possible. Data recorders were placed in the four major coastal water bodies of the estuary (ES1, ES2, WESC, and Dudley Pond; fig 4.2). Continuous discharge values were calculated at the outlet channel of the east estuary. Finally, discharge at Bosco Creek, the primary surface-water inflow source to the east estuary, was periodically measured during the study to characterize surface-water fluxes.

Salinity, Temperature, and Depth Measurements in the Estuary

Water-temperature and salinity data were collected with self-recording electrical conductivity and temperature (CT) sensors, some of which also included transducers to measure water depth (CTD). These sensors were placed at four locations throughout the estuary (fig. 4.2; table 4.1). The sensors were attached to steel rods pounded into the estuary substrate and sampled at 15-minute or 1-hour intervals. The CTDs were in ES2 from June 2008 to April 2010, and in Dudley Pond from May 2009 to April 2010 (table 4.1). The CTs were placed in ES1 from July 2007 to March 2010, and in the WESC from May 2009 to April 2010 (table 4.1). Salinity data are presented in Practical Salinity Units (PSU), which is a relative salinity scale approximately equivalent to the total mass of salts in parts per thousand. Ocean water and freshwater typically are about 32 and 0 PSU, respectively.

Water levels in Dudley Pond and ES2 correlate with tidal fluctuations in the Strait of Juan de Fuca, represented by the water level at the NOAA tide gage in Port Angeles, Washington (fig. 4.16). However, water-level oscillations in Dudley Pond were smaller than ES2, and there was a lag in time between the water levels at Port Angeles and in Dudley Pond (fig. 4.16*A*). In contrast, the water level in ES2 correlates well with the high tides in the Strait of Juan de Fuca (fig. 4.16*B*), suggesting a direct surface-water connection with the river mouth.

Salinity levels in Dudley Pond were fairly low and steady, while WESC, on the river side of the levee, had higher levels and more fluctuations of salinity, suggesting more mixing of freshwater and seawater in WESC than in Dudley Pond (fig. 4.16). The east estuary (ES1 and ES2) had greater oscillations in salinity than the west estuary. Near the outlet of the estuary (ES1), there were daily oscillations between almost pure freshwater (about 0 PSU) and almost pure seawater (about 32 PSU). In ES2, salinity values commonly reached only one-third to one-half of those found in ES1 (fig. 4.16).

A longer record (spring to autumn 2009) of water temperature and salinity from the CTDs also demonstrated the differences between Dudley Pond on the west side and ES2 in the eastern estuary (fig. 4.17). During this sampling interval, there was a general warming trend until August, followed by a cooling trend through December. Dudley Pond was commonly from 2 to 5 °C warmer than ES2 during the summer (fig. 4.17A). The salinity levels in ES2 were more variable, and reached higher levels, than salinity levels in Dudley Pond (figs. 4.17*B* and 4.18).

Figure 4.15. Effects of tides on water levels in the Elwha River mouth and estuary, Washington. The date, time, and tidal stage, measured in meters above Mean Lower Low Water (MLLW) at National Oceanic and Atmospheric Administration tidal station 9444090 in Port Angeles, is shown for each photograph. (Photographs taken by Ian M. Miller (*E* and *F*) and Patrick B. Shafroth.)

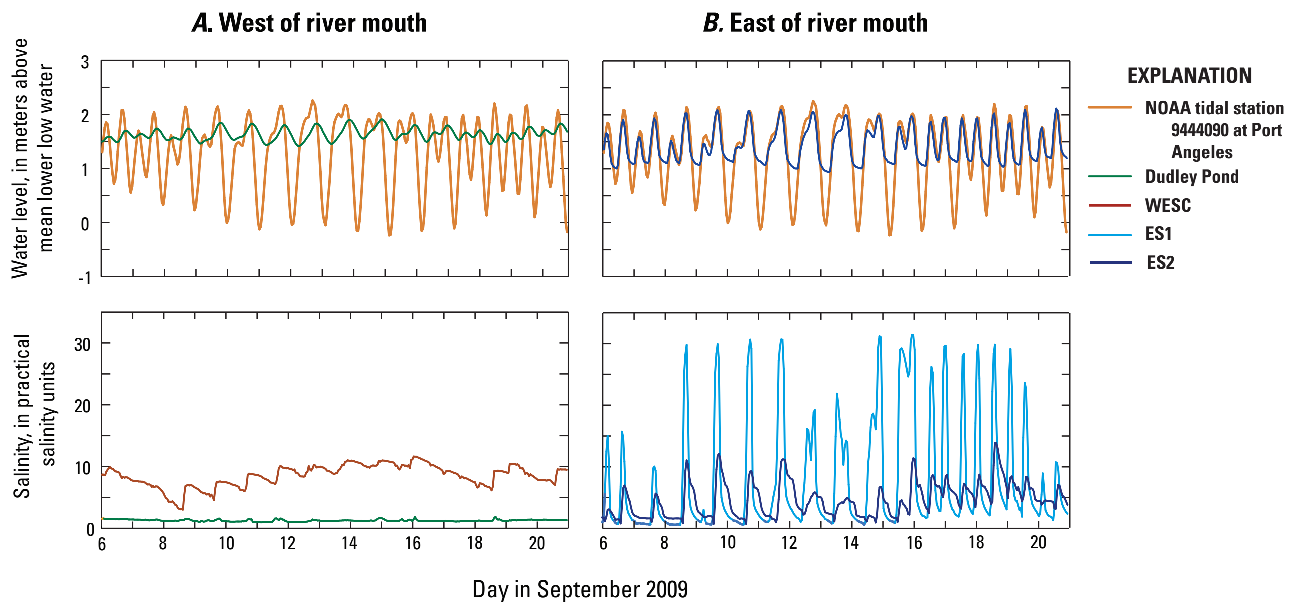

Figure 4.16. Surface-water levels and salinity over a 2-week (spring-neap) tidal cycle during low flow for (*A*) Dudley Pond and WESC in the west estuary and (*B*) ES1 and ES2 in the east estuary of the Elwha River, Washington, September 2009.

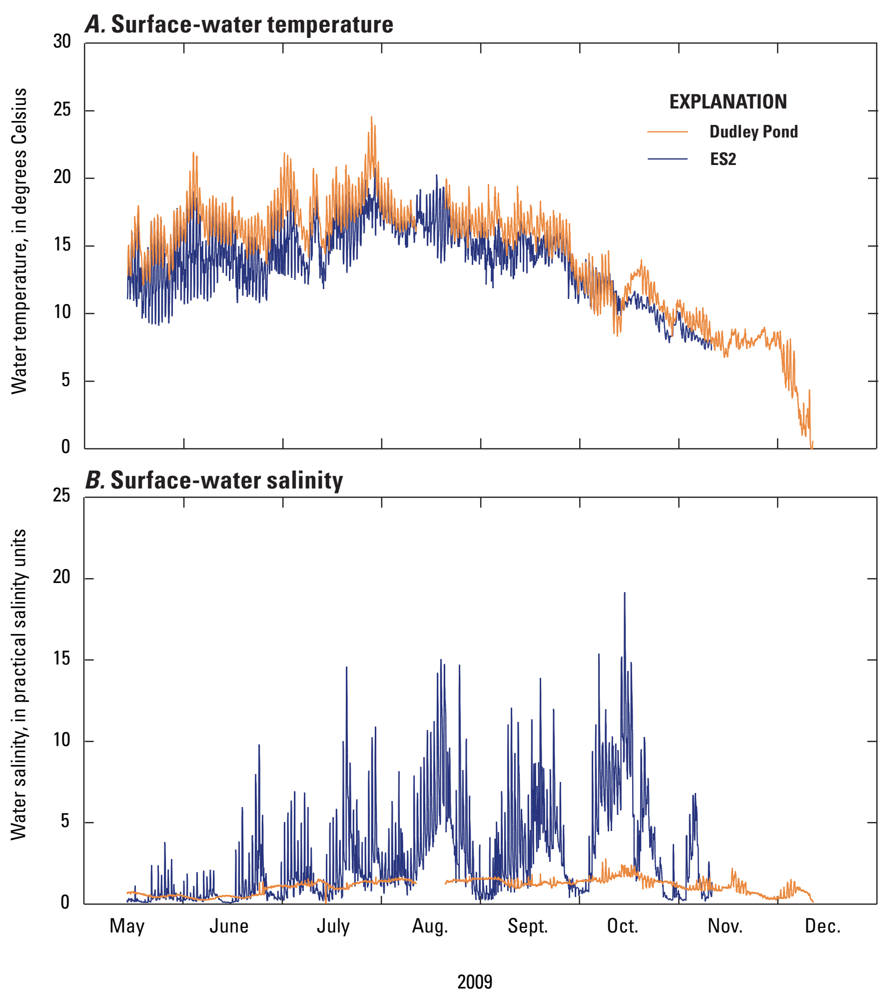

Figure 4.17. Surface-water (*A*) temperature and (*B*) salinity in Dudley Pond (west estuary) and ES2 (east estuary) in the Elwha River estuary, Washington, May–December 2009. Dudley Pond is consistently warmer, but it does not receive estuarine mixing during spring tides like ES2.

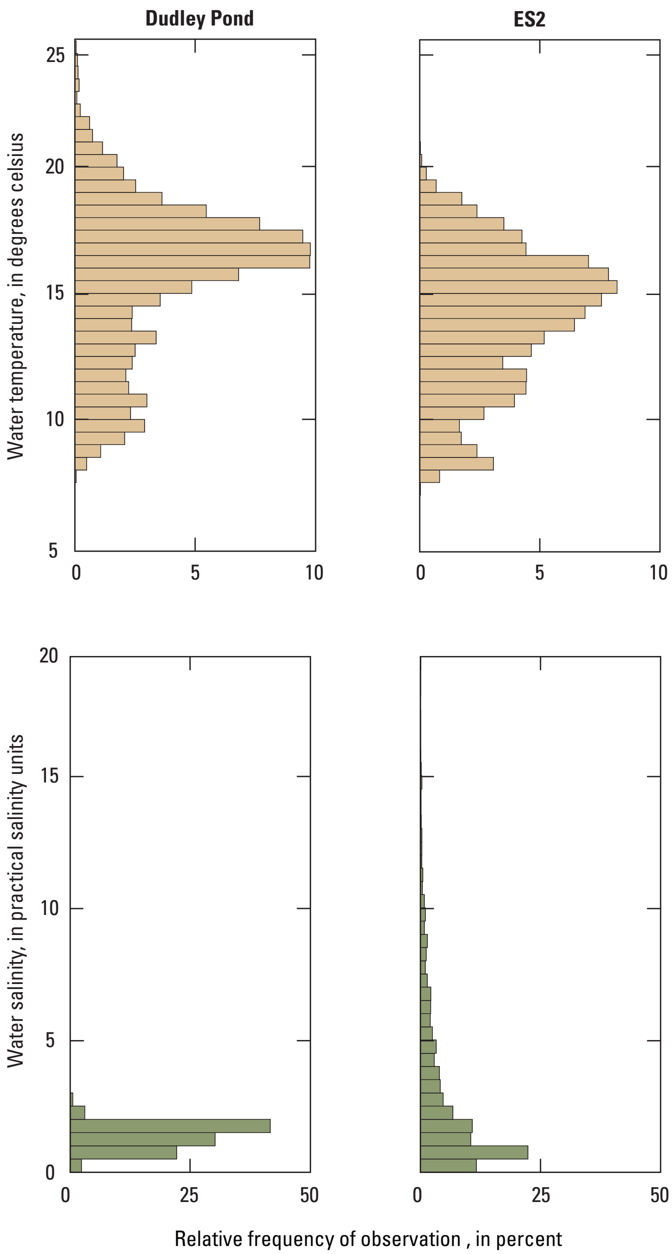

Figure 4.18. Frequency distribution plots showing comparison of water temperatures and salinities in Dudley Pond and ES2 in the Elwha River estuary, Washington, from May 14, 2009, to November 10, 2009.

Surface-Water Temperature Measurements in the East Estuary

To further characterize the temperature of surface water in the east estuary, six temperature data recorders were deployed in surface-water sites distributed throughout the estuary (fig. 4.2; table 4.1). These deployments started in early August 2009 during a cycle of large tidal variability. The six thermal recorders measured near-benthic temperature and the data helped explain overall spatial and temporal thermal trends in estuarine water. One “transect” of sensors was placed approximately parallel to the shoreline and included TStn 4 to the west, TStn 6 in ES1, and TStn 5 in Bosco Creek near where the creek enters ES2 (fig. 4.2). Another sensor transect was placed north-south in “finger” channels of ES2 (TStn 3 and TStn 2), and a secondary surface-water body to the south of ES2 (TStn 1; fig. 4.2). TStn 4, 5, and 6 were removed on August 8, 2009. TStn 1, 2, and 3 were removed in December 2009.

For thermal-recorder deployments, posts were pounded into the substrate of the bed of the water body, and a slotted plastic pipe was attached to the post. The bottom of the plastic pipe was positioned about 5 cm above the estuary substrate. The thermal recorders were placed near the bottom of the plastic pipe and secured with a nylon string hung from a bolt inserted near the top of the plastic pipe. TStn 4 was placed in a shallow well dug into the subaqueous substrate with a slotted-plastic casing. All thermal recorders were synchronized and recorded data at 15-minute intervals.

Overall, the thermal recorders operating in the east estuary showed diurnal fluctuations in temperature and a general cooling trend from summer into autumn and early winter (fig. 4.19). Additional temperature data collected at the Port Angeles tidal station (NOAA 9444090) showed that water temperature in the east estuary was closely coupled to seasonal air temperature, but was largely independent from marine water temperature in the Strait of Juan de Fuca. From August 3, 2009, to August 8, 2009, the lowest temperatures and the largest diurnal fluctuations were at TStn 5 (located where Bosco Creek enters ES2; fig. 4.2). Similarly, the next lowest recorded temperature values in the east estuary were measured at TStn 4, closest to the outlet channel (fig. 4.2). Diurnal temperature variation decreased from the summer months to the autumn.

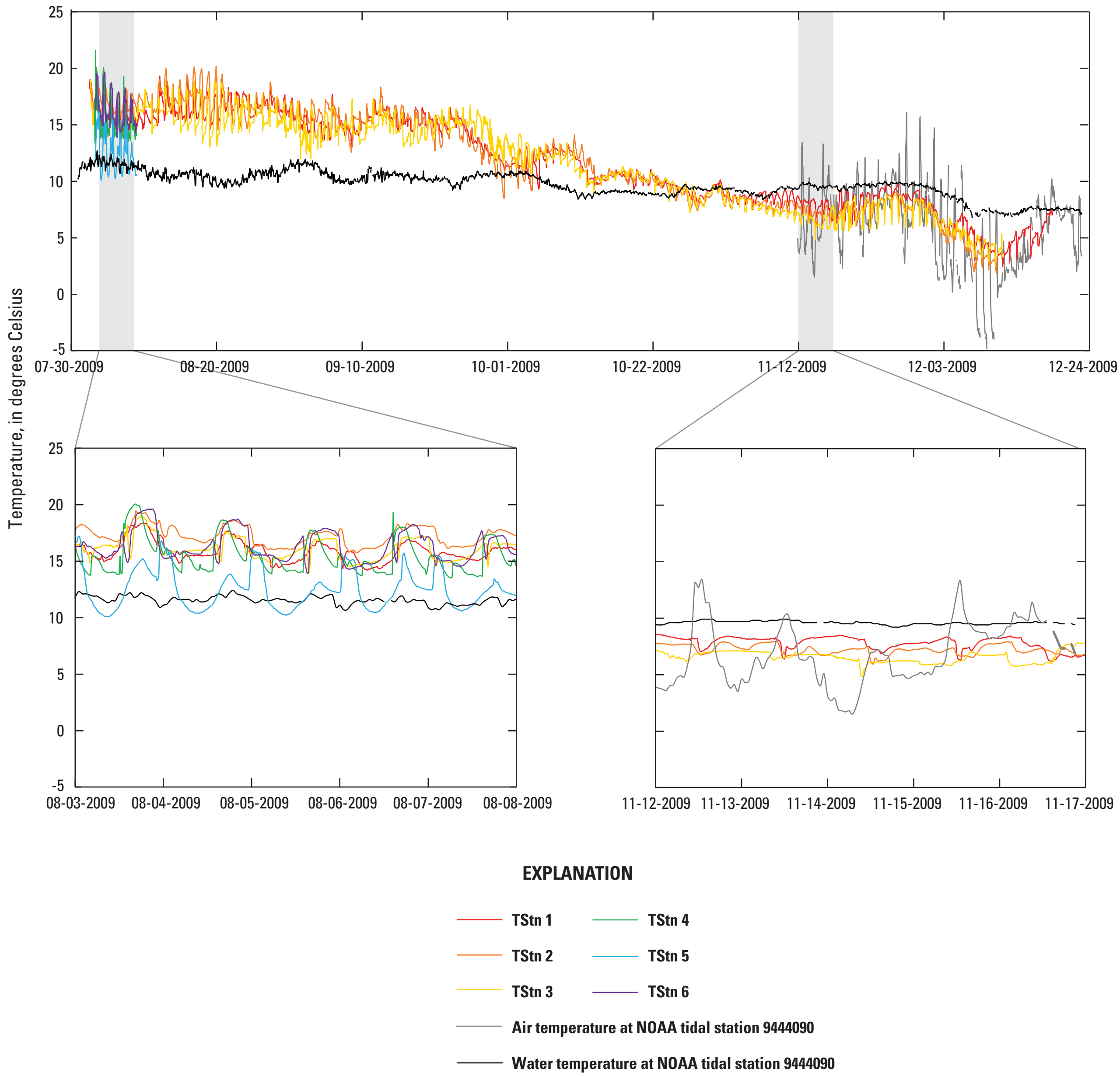

Figure 4.19. Surface-water temperature data collected in the eastern estuary of the Elwha River, Washington, July–December 2009.

Surface-Water Movement in the Estuary

To understand and quantify the flux of surface water to and from the east estuary, water velocity and depth were monitored in the ES1 outlet channel from June 3 to 13, 2008, and from August 3 to September 2, 2008. A 3-MHz acoustic Doppler velocity meter was mounted to the bottom of the ES1 outlet channel (fig. 4.2), and water velocity, stage, and temperature were recorded at 5-minute intervals. During the period of continuous acoustic Doppler velocity meter operation, discrete discharge and channel-geometry measurements were made at the ES1 outlet channel over incoming and outgoing flows, and used to develop index-velocity and stage-area relations needed to compute a continuous discharge record at the site. Positive discharge was defined as flow out of the east estuary; negative discharge as flow into the east estuary.

On four occasions during summer 2008 (June 3, June 13, July 16, and August 3), instantaneous discharge was measured at the Bosco Creek gaging station (12046523). In addition to periodic flow measurements, stage in Bosco Creek was continuously monitored during the study period with a 5-psi non-vented transducer, which was corrected for atmospheric pressure changes using a collocated barometric pressure recorder.

From June 3 to 13, 2008, the average net discharge of water from the ES1 outlet channel was 0.26 m^3/s. Surface-water discharge into the estuary from Bosco Creek was 0.09 and 0.08 m^3/s on June 3 and 13, respectively. The stage record at Bosco Creek showed a gradual decrease in stage during this period. Assuming that precipitation and evapotranspiration losses from the estuary were small, the Bosco Creek contribution accounted for about one-third of net surface-water flow to the estuary. The net discharge from the ES1 outlet channel was calculated to be 0.12 m^3/s for the sampling period August 3 to September 2, 2008. Average discharge from Bosco Creek, measured on July 16 and August 3, was 0.04 m^3/s, about one-third of the total net flux at the ES1 outlet channel in July and August. These results suggest that most of freshwater contributions to the estuary were from hyporheic flow, a mixture of shallow groundwater and subsurface river flow originating upstream and discharging into the estuary system. Overall, the discharge measurements at the ES1 outlet channel ranged from -0.30 to 1.12 m^3/s, demonstrating the close connection between tidal potential and surface-water from the estuary.

A 2-week record of these measurements in August 2008 shows the cyclical nature of water flux at the estuary outlet (fig. 4.20). The discharge of water into ES1 (vertical shading; fig. 4.20) occurred over a shorter duration, and at a smaller rate, than outflow. The resulting net discharge exiting ES1 to the river averaged about 14,000 m^3/d, or 0.17 m^3/s for the period recorded. Instantaneous peak discharge during rising-tide conditions exceeded 2 m^3/s, which is more than 10 times the net flow rate. This net outflow through the ES1 outlet channel represented the relative contributions of surface-water flow from Bosco Creek and groundwater flow into the estuary.

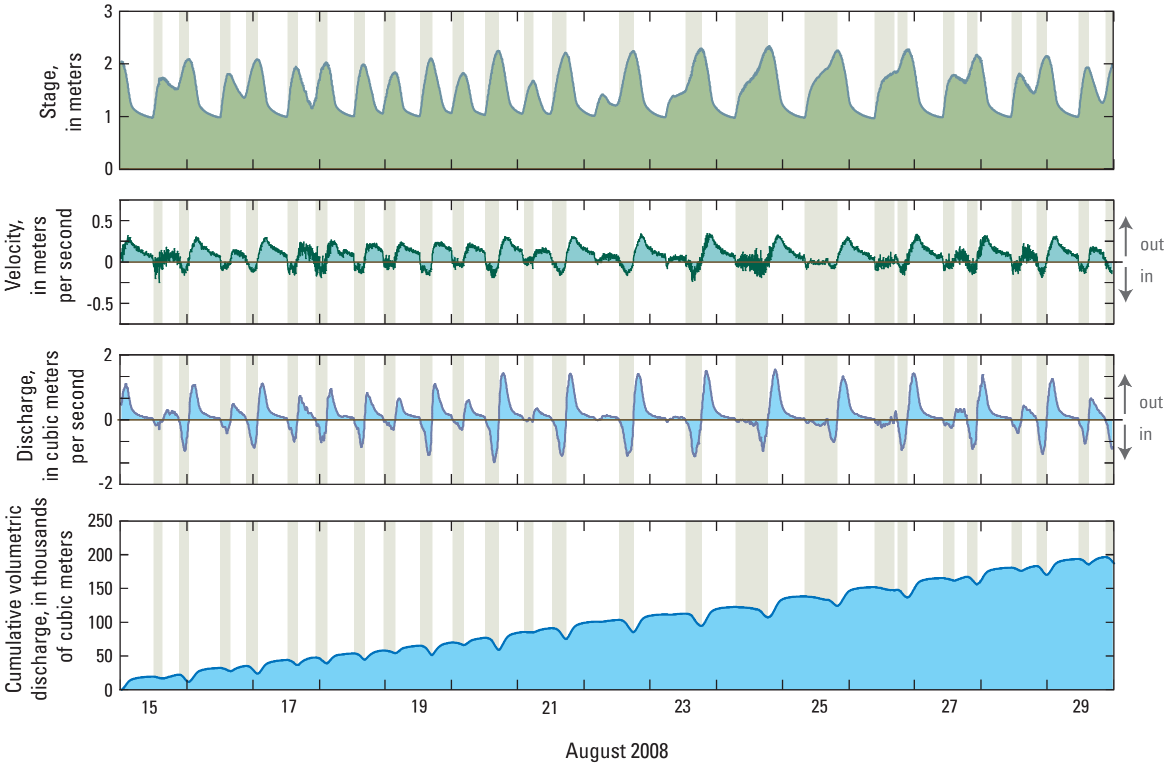

Figure 4.20. Measured stage, velocity, and discharge of water into and out of the east estuary through the ES1 outlet channel in the Elwha River estuary, Washington, during 2 weeks in August 2008. Shaded vertical bands show intervals of time with inflow into the estuary. The average net outflow was about 14,000 cubic meters per day (0.17 cubic meters per second).

Synthesis of Estuarine Hydrologic Data

Integrating the salinity, temperature, depth, and discharge data collected during this study allows insight into water movement and exchange in estuarine water bodies. During much of the year, water response in the estuary is governed by tidal cycles and groundwater and surface-water input from the aquifer and river. When storms affect the region, waves at the shoreline and high discharge within the river can alter estuarine water conditions for days or weeks.

General Water Movement within the Estuary Complex

The observations of water level, temperature, and salinity from the sensor network showed how hydrologic conditions varied across the estuary. For example, water level and salinity from measurements west and east of the river mouth revealed contrasting conditions during the summer of 2009. Although water levels in Dudley Pond and ES2 responded to tidal fluctuations in the Strait of Juan de Fuca, water level oscillations in Dudley Pond were smaller than ES2 (fig. 4.16). Furthermore, the western flood-control levee had hydraulically isolated Dudley Pond from direct connection with the river and Strait of Juan de Fuca, which limited water exchange to groundwater seepage and direct overwash of the beach berm from large waves. Groundwater exchange was responsible for most of the fluctuations in Dudley Pond water levels, shown by the lag between the water levels in the Strait of Juan de Fuca and in Dudley Pond (fig. 4.16*A*); in contrast, ES2 had a direct surface-water connection with the river mouth, shown by the close correlation in stage during the higher tides in the Strait of Juan de Fuca (fig. 4.16*B*).

These different hydrologic settings across the estuary also influenced the mixing of seawater throughout this system, shown by the substantial differences in the values and patterns of salinity across measurement sites. Dudley Pond, which was not connected to the Strait of Juan de Fuca by surface-water, had lower and more constant salinity, as opposed to WESC, on the river side of the levee, where there was more mixing of freshwater and seawater than in Dudley Pond (figs. 4.16 and 4.17). Similarly, the greater summer warming in Dudley Pond as compared to ES2 (fig. 4.17) also suggested a lack of surface-water connection to Dudley Pond.

Within the WESC, high water levels in the Strait of Juan de Fuca induced rapid increases of salinity which then decreased somewhat steadily until the next high water. This freshening effect between high waters likely was from hyporheic input. The greater oscillations in salinity in the east estuary (ES1 and ES2) resulted from tidal flows through the ES1 outlet channel (fig. 4.16). The spatial gradient in salinity values from ES1 to ES2 (greater daily oscillations in ES1 than ES2; fig. 4.16), demonstrated that the entire east estuary did not fully flush during each tidal cycle.

Surface-water temperatures in the eastern estuary (ES1 and ES2) followed the general decreasing trends measured in Dudley Pond (fig. 4.19). Diurnal variation in temperature also was greater in the summer months when clear skies allowed greater solar heating during the day and enhanced radiative cooling at night. As climatic temperatures decreased in the autumn, increased cloud cover reduced radiative heat transfer and diurnal temperature variation decreased. The cooler Bosco Creek temperatures (TStn 5; fig. 4.19) reflected the influence of spring-fed surface waters flowing down the creek. Near the outlet channel (fig. 4.2), temperatures were lower in TStn 4 and therefore were more strongly influenced by fluxes into the estuary from the river (fig. 4.19).

Different distributions of water temperature and salinity were measured within the 1 km that separates ES2 in the east estuary from Dudley Pond (fig. 4.18). Dudley Pond was warmer and less brackish than ES2. These differences were directly related to unique circulation patterns in the two water bodies, particularly the absence of hydraulic connection of surface water to Dudley Pond. Similarly, substantial differences were observed in fish diversity and abundance, invertebrate community composition, and vegetation structure between the east and west estuary (Shaffer and others, 2009; Duda and others, 2011a, chapter 7, this report; Shafroth and others, 2011, chapter 8, this report).

Effects of River Flooding and Morphologic Changes on Estuarine Hydrology

Heavy precipitation and snow melt create high discharge and stage on the lower Elwha River. Stage at the mouth of the Elwha River also rises during high tides, and these temporary changes in water levels influence water movement throughout the estuary.

The effects of the December 2007 peak-flow event, with a maximum value of 1,020 m^3/s and an estimated 40-year recurrence interval (Draut and others, 2011), were recorded in measurements in the east estuary. The high river flow lasted 2 days during which time the water levels in ES1 remained uncharacteristically high (fig. 4.21). The event reduced salinity in ES1 to nearly 0 PSU for 2 weeks, even though the pattern of fluctuation in stage in ES1 was strongly forced by tidal cycles immediately after this event (fig. 4.22).

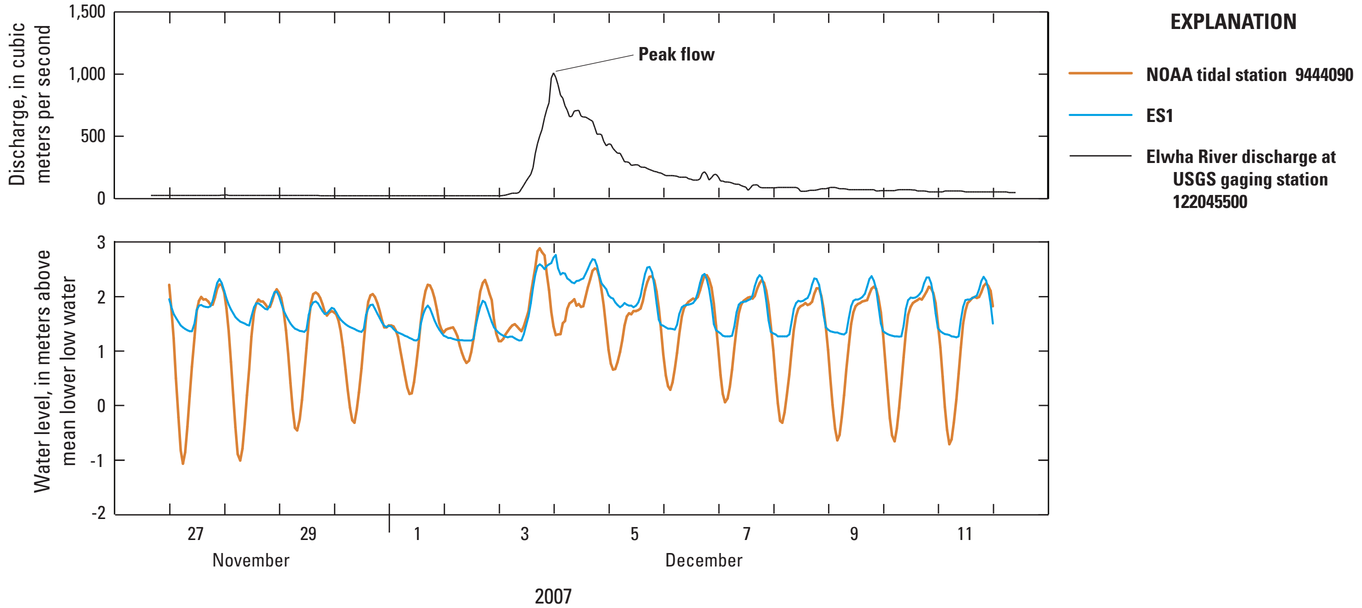

Figure 4.21. Discharge, stage in ES1 measured in the Elwha River, and tidal stage measured at National Oceanic and Atmospheric Administration (NOAA) tidal station 9444090 in Port Angeles, Washington, during the large peak-flow event of December 2007.

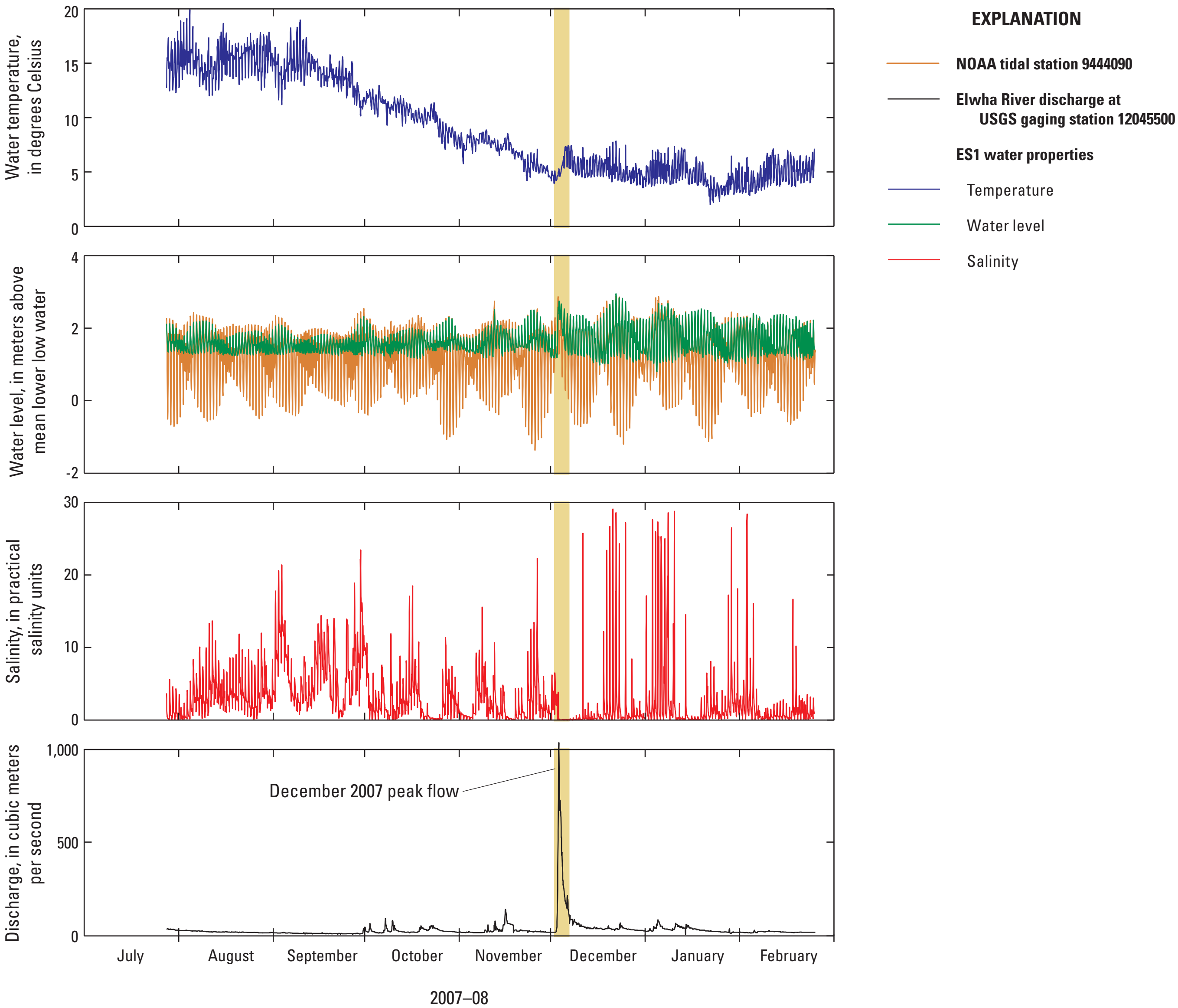

Figure 4.22. Hydrologic, temperature, and salinity conditions in the east estuary (ES1) related to the discharge in the Elwha River, Washington, from August 2007 to February 2008. The effects of the December 2007 peak-flow event on the east estuary are apparent, with decreased salinity in the east estuary for 2 weeks, and increased water levels and temperature.

This peak-flow event also modified the surface-water connection between the river mouth and ES1. During the event, 7–8 m of bank erosion and channel migration occurred in the river adjacent to the east estuary (Draut and others, 2011). This morphologic change altered the size and elevation of the ES1 outlet channel, increasing the hydraulic connection between the river and ES1. These changes were reflected in the increased amplitude of water levels in ES1 after the event (fig. 4.22). After the 2007 peak-flow event, there was approximately 1 m greater range in the cycle of stage in ES1; the stage peaks were higher, and the stage troughs were lower (fig. 4.23). Similarly, water salinity in ES1 had more variability following the 2007 peak-flow event, further reflecting larger overall volumetric exchange of water through the ES1 outlet channel (fig. 4.22).

Although the December 2007 peak-flow event expanded the ES1 outlet channel, future high flows or channel reorganization might reduce the size of this connecting channel or block it altogether. Such a cut-off event would greatly reduce estuarine exchanges in ES1 and ES2, dampening fluctuations in water level, temperature, and salinity to levels currently observed in the WESC or Dudley Pond. A blockage also would limit access to rearing habitat for young fish. For example, a large sediment deposit completely blocked access to ES1 and ES2 following a peak-flow event in November 2006. This particular estuary blockage changed the community composition and density of salmonids in 2007 (Duda and others, 2011a, chapter 7, this report).

Conceptual Model of Water Exchange in the Estuary

The observations of water conditions and flow from 2007 to 2009 provided insight into the general framework of water exchange within the river mouth and estuary. The extent and timing of these water exchanges are related to the connections of surface water and groundwater to these water bodies, and it is apparent, for the east estuary at least, that these surface-water connections can change dramatically after high flows or by channel-evolution processes.

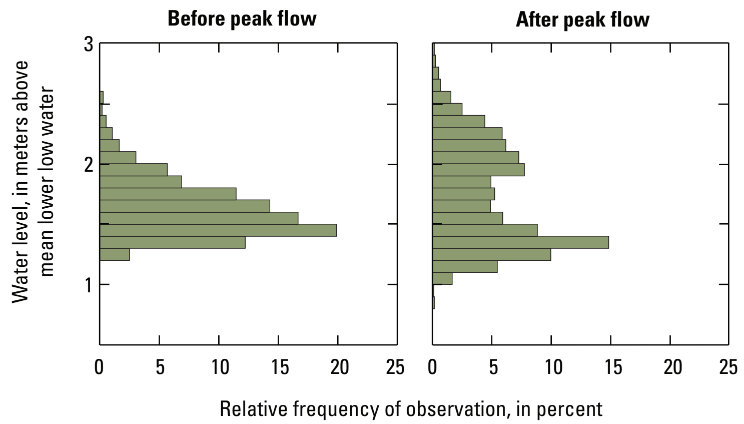

Figure 4.23. Frequency distribution plots showing a comparison of water levels in ES1, in the east estuary of the Elwha River, Washington, for the 80 days before (September 7, 2007, to November 29, 2007) and after (December 8, 2007, to February 25, 2008) the large river peak-flow event of December 2007. The wider distribution of water levels after the peak-flow event indicates an increase in the surface-water connectivity between the tidal river mouth and east estuary.

A conceptual diagram (fig. 4.24) schematically shows the movement of water through the estuary over a tidal cycle under the current pre-dam-removal conditions. Water movement, in turn, affects salinity patterns and overall water quality in the estuary (fig. 4.24). Between high and low tide, the river exports water through the river mouth. The river discharge rate and evacuation from ES1 and ES2 is greatest during the falling (ebbing) tide (fig. 4.24*B*). During the rising (flooding) tide, saline ocean water enters the river mouth and spreads into connecting estuarine channels causing increases in water salinity within the estuary (fig. 4.24*D*). The rate of water flux through these estuarine channels is governed by geometry in the ES1 outlet channel and stage in ES1, ES2, and the river. Moreover, overall magnitude of estuarine-channel water flux changes with the regular morphologic evolution of the river-mouth region (Warrick and others, 2011a, chapter 3, this report). With the imminent removal of the two dams on the Elwha River and the arrival of increased sediment load and concomitant morphological changes, the Elwha River estuary likely will experience a dynamic increase in the rate of change and evolution. At some point after dam removal, when the fluvial transport of sediment and large woody debris stabilizes, the rate of morphological change in the estuary would, presumably, reach a new equilibrium.

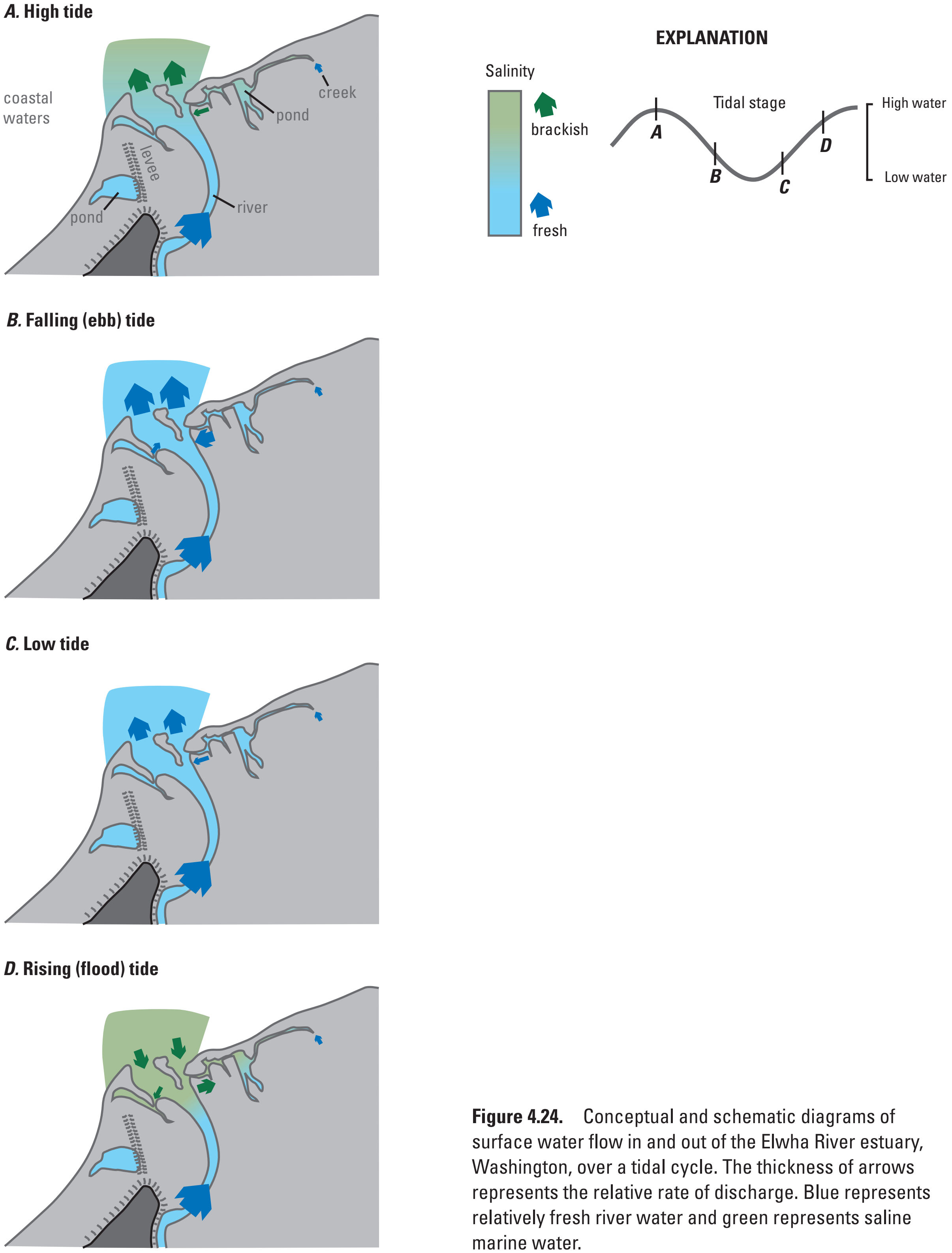

Figure 4.24. Conceptual and schematic diagrams of surface water flow in and out of the Elwha River estuary, Washington, over a tidal cycle. The thickness of arrows represents the relative rate of discharge. Blue represents relatively fresh river water and green represents saline marine water.

Summary

To better understand the hydrology of the lower Elwha River and its estuary before the removal of two dams, the U.S. Geological Survey, working with collaborators, collected baseline hydrologic data and interpreted the current hydrologic state of the lower-river system. In particular, transient storage was measured in the lower river, groundwater response and river interactions with the groundwater aquifer were characterized, salinity and stage were measured and analyzed in estuarine water bodies, and the movement of water through the estuary was analyzed and characterized.

Transient storage has been measured in many streams throughout the United States; however, due to logistical constraints, these studies are typically conducted on small headwater streams. Relatively few transient-storage studies have been conducted on larger systems comparable to the Elwha River or used to quantify changes in transient storage following a large dam removal, although theoretical models have predicted how a channel will change after small dam removals. Results from this study represent a unique dataset to assess changes in a large river before and after dam removal and the subsequent effects on channel shape and sediment supply. The dye experiment showed that the low-flow channel of the lower 3.9 kilometers of the Elwha River was relatively simple, and 1 to 6 percent of the median travel time of dye was attributed to transient-storage processes.

The monitoring of groundwater elevation in four wells located along the lower Elwha River showed a strong correlation between stage in the river and groundwater levels in the flood plain. A tidal signal also was observed in the groundwater-elevation data, but groundwater fluctuations from tides were significantly smaller than fluctuations due to changes in river stage. Water temperature data collected in the monitoring wells showed a delay of days to months between the changes in temperature in the well adjacent the river and temperature in wells farther from the river.

A seepage investigation along the lower 4.4 kilometers of river in September 2007 showed a 10 percent loss of river flow to the groundwater aquifer at a section of the river 1.7 to 2.8 kilometers upstream of the mouth. No clear trends of losses or gains were observed along the rest of the study reach.

A distributed temperature sensing cable deployed for 20 hours in the east estuary on September 1–2, 2008, characterized bed temperature of ES2, ES1, the main-stem river, and the interconnecting channels of the east estuary. Both ES1 and ES2 were warmed by solar heating during the day, and the water temperature in ES2 remained a relatively constant 14 to 15 °C. ES1 was cooled during the day and night as tidally influenced water from the river flowed into the estuary. ES2 remained relatively warm during the night hours due to its distance from the river and larger size. An analysis of the temperature variance at particular points along the cable enabled the identification of one pronounced location in the middle of ES1 where groundwater upwelling regulated the temperature of the estuary bed. The location probably is an old relict river channel. Two other possible upwelling sites were located along the cable, although the variance data could not conclusively confirm these upwelling sites.

Salinity and depth data were collected at locations in ES1, ES2, the WESC, and Dudley Pond from 2007 to 2010 helping to explain how water moved through the estuary. During summer low-flow conditions in the river, stage and salinity in ES1 and ES2 were found to fluctuate significantly in response to the rising (flooding) and falling (ebbing) tides. Salinity in ES1 in September 2009 ranged between 1 and 32 Practical Salinity Units (PSU), and salinity in ES2 ranged between 1 and 15 PSU. In contrast, fluctuations of stage and salinity in the WESC were much less pronounced. Salinity in the WESC ranged between about 3 and 11 PSU. Changes in stage were relatively small in Dudley Pond, reflecting the fact that this water body is hydraulically isolated from the river and the Strait of Juan de Fuca. Similarly, salinity in Dudley Pond was no more than 2 PSU during the low-flow conditions of late summer 2009. As the estuary was influenced by storm conditions in autumn and winter, overall salinity as well as salinity fluctuations increased in the estuary. In contrast, temperature and temperature fluctuations decreased as the weather became dominated by temperate rain storms and cloudy conditions.

An acoustic Doppler velocity meter deployed in the ES1 outlet channel in the summer of 2008, coupled with discharge and stage measurements, allowed the measurement of the total discharge of surface water flowing from the east estuary. Although discharge moved both in and out of the estuary, depending on river stage governed by tidal cycles, the net flow of surface water was out of the east estuary. In June, the net outflow from the east estuary averaged 0.26 m^3/s. In August and September, the net outflow averaged 0.12 m^3/s. Contemporaneous measurements of discharge in Bosco Creek showed that the surface-water inflow into the east estuary was about one-third the net outflow through the ES1 outlet channel, both in June and in August to September. It was presumed that the remaining two-thirds of extra inflow originated from groundwater flow into the estuary.

The river's influence on estuarine salinity and stage increased dramatically in autumn and winter as peak-flow

events in the main-stem river, coupled with tidal effects, pushed large volumes of fresh water into the east estuary. For example, a large peak-flow event in the river in December 2007 reduced salinity in ES1 to nearly zero for two weeks.

The data collected within and adjacent to the estuary helped to explain some of the complex interactions of saline marine water, fresh river water, and fresh groundwater under seasonal conditions. This insight led to the formulation of a simple conceptual model of water movement in the estuary that will help guide future research efforts focused on understanding river and estuary response to dam removal.

The underlying hydrologic framework of the lower Elwha River, its mouth, and the estuarine system of coastal ponds and interconnected channels reflects a complex set of fluvial, marine, geologic, climatic, and anthropogenic influences. These hydrologic processes will likely change after the removal of the two, long-standing Elwha River dams. Although the opportunity to study and understand the evolution of these hydrologic processes during and after dam removal is unprecedented, the collection of baseline hydrologic data and the formulation of fundamental scientific understanding of the existing processes are essential to maximize the potential insight gained from a dam-removal project of exceptional size and complexity.

This chapter documents efforts by the U.S. Geological Survey and its collaborating partners to monitor and interpret the hydrologic system within the lower Elwha River and its estuary. More importantly, the basic research characterizing the hydrologic framework of the dam-influenced Elwha River contained herein will provide future scientists the opportunity to study processes and river and estuary responses not envisioned before the project.

Acknowledgments

Michael McHenry, Matthew Beirne, Mitch Boyd, all with the Lower Elwha Klallam Tribe, contributed expertise, advice, and data to support this study.

References Cited

Bencala, K.E., and Walters, R.A., 1983, Simulation of solute transport in a mountain pool-and-riffle stream—A transient storage model: Water Resources Research, v. 19, p. 718-724.

Boano, F., Camporeale, C., Revelli, R., and Ridolfi, L., 2006, Sinuosity-driven hyporheic exchange in meandering rivers: Geophysical Research Letters, v. 33, L18406, 4 p.

Bukaveckas, P.A., 2007, Effects of channel restoration on water velocity, transient storage, and nutrient uptake in a channelized stream: Environmental Science and Technology, v. 41, p. 1570-1576.

Butturini, A., and Sabater, F., 1999, Importance of transient storage zones for ammonium and phosphate retention in a sandy-bottom Mediterranean stream: Freshwater Biology, v. 41, p. 593-603.

Connolly, P.J., and Brenkman, S.J., 2008, Fish assemblage, density, and growth in lateral habitats within natural and regulated sections of Washington's Elwha River prior to dam removal: Northwest Science, v. 82 (special issue), p. 107-118.

Curran, C.A., Konrad, C.P., Dinehart, R.L., and Moran, E.H., 2008, Bank topography, bathymetry, and current velocity of the lower Elwha River, Clallam County, Washington, May 2006: U.S. Geological Survey Data Series 363, 11 p. (Also available at http://pubs.usgs.gov/ds/363/.)

Czuba, C.R., Randle, T.J., Bountry, J.A., Magirl, C.S., Czuba, J.A., Curran, C.A., and Konrad, C.P., 2011, Anticipated sediment delivery to the lower Elwha River during and following dam removal, chap. 2 *of* Duda, J.J., Warrick, J.A., and Magirl, C.S., eds., Coastal habitats of the Elwha River, Washington—Biological and physical patterns and processes prior to dam removal: U.S. Geological Survey Scientific Investigations Report 2011-5120, p. 27-46.

Draut, A.E., Logan, J.B., and Mastin, M.C., 2011, Channel evolution on the dammed Elwha River, Washington, USA: Geomorphology, v. 127, p. 71-87, doi:10.1016/j.geomorph.2010.12.008.

Duda, J.J., Freilich, J.E., and Schreiner, E.G., 2008, Baseline studies in the Elwha River ecosystem prior to dam removal—Introduction to the special issue: Northwest Science, v. 82 (special issue), p. 1-12.

Duda, J.J., Beirne, M.M., Larsen, K., Barry, D., Stenberg, K., and McHenry, M.L., 2011a, Aquatic ecology of the Elwha River estuary prior to dam removal, chap. 7 *of* Duda, J.J., Warrick, J.A., and Magirl, C.S., eds., Coastal habitats of the Elwha River, Washington—Biological and physical patterns and processes prior to dam removal: U.S. Geological Survey Scientific Investigations Report 2011-5120, p. 175-224.

Duda, J.J., Warrick, J.A., and Magirl, C.S., 2011b, Coastal and lower Elwha River, Washington, prior to dam removal—History, status, and defining characteristics, chap. 1 *of* Duda, J.J., Warrick, J.A., and Magirl, C.S., eds., Coastal habitats of the Elwha River, Washington—Biological and physical patterns and processes prior to dam removal: U.S. Geological Survey Scientific Investigations Report 2011-5120, p. 1-26.

Ely, D.M., Frasl, K.E., Marshall, C.A., and Reed, F., 2008, Seepage investigation for selected river reaches in the Chehalis River basin, Washington: U.S. Geological Survey Scientific Investigations Report 2008-5180, 12 p.

Fitzpatrick, F.A., Waite, I.R., D'Arconte, P.J., Meador, M.R., Maupin, M.A., and Gurtz, M.E., 1998, Revised methods for characterizing stream habitat in the national water-quality assessment program: U.S. Geological Survey Water-Resources Investigations Report 98-4052, 67 p.

Gooseff, M.N., Anderson, J.K., Wondzell, S.M., LaNier, J., and Haggerty, R., 2006, A modeling study of hyporheic exchange pattern and the sequence, size, and spacing of stream bedforms in mountain stream networks, Oregon, USA: Hydrological Processes, v. 20, p. 2443-2457.

Gooseff, M.N., Hall, Jr., R.O., and Tank, J.L., 2007, Relating transient storage to channel complexity in streams of varying land use in Jackson Hole, Wyoming: Water Resources Research, v. 43, W01417 10 p.

Harvey, J.W., and Wagner, B.J., 2000, Quantifying hydrologic interactions between streams and their subsurface hyporheic zones, *in* Jones, J.B, and Mulholland, P.J., eds., Streams and ground waters: San Diego, Academic Press, p. 1-44.

Harvey, J.W., Conklin, M.H., and Koelsch, R.S., 2003, Predicting changes in hydrologic retention in an evolving semi-arid alluvial stream: Advances in Water Resources, v. 26, p. 939-950.

Keddy, P., 2000, Wetland ecology—Principles and conservation: Cambridge, U.K., Cambridge University Press, 614 p.

Kilpatrick, F.A., and Cobb, E.D., 1985, Measurement of discharge using tracers: U.S. Geological Survey Techniques in Water Resources Investigations, book 3, chapter A16, 52 p. (Also available at http://pubs.usgs.gov/twri/twri3-a16/.)

Kilpatrick, F.A., and Wilson, J.F., Jr., 1989, Measurement of time of travel in streams by dye tracing: U.S. Geological Survey Techniques of Water Resources Investigations, book 3, chapter A9, 52 p. (Also available at http://pubs.usgs.gov/twri/twri3-a9/.)

Kloehn, K.K., Beechie, T.J., Morley, S.A., Coe, H.J., and Duda, J.J., 2008, Influence of dams on river-floodplain dynamics in the Elwha River, Washington: Northwest Science, v. 82 (special issue), p. 224-235.

Mitsch, W.J., and Gosselink, J.G., 1993, Wetlands (2nd ed.): New York, N.Y., Van Nostrand Reinhold, 722 p.

Mueller, D.S., and Wagner, C.R., 2009, Measuring discharge with acoustic Doppler current profilers from a moving boat: U.S. Geological Survey Techniques and Methods 3A-22, 72 p.

Mulholland, P.J., Marzolf, E.R., Webster, J.R., Hart, D.R., and Hendricks, S.P., 1997, Evidence that hyporheic zones increase heterotrophic metabolism and phosphorus uptake in forest streams: Limnology and Oceanography, v. 42, p. 443-451.

Pacific Groundwater Group, 2005, Evaluation of groundwater levels in the lower Elwha River valley: Report prepared for the Lower Elwha Klallam Tribe, September 30, 2005, 24 p.

Runkel, R.L., 1998, One-dimensional transport with inflow and storage (OTIS)—A solute transport model for streams and rivers: U.S. Geological Survey Water Resources Investigations Report 98-4018, 73 p.

Runkel, R.L., 2002, A new metric for determining the importance of transient storage: Journal of the North American Benthological Society, v. 21, p. 529-543.

Selker, J.S., Thévenaz, L., Huwald, H., Mallet, A., Luxemburg, W., van de Giesen, N., Stejskal, M., Zeman, J., Westhoff, M., and Parlange, M. B., 2006, Distributed fiber-optic temperature sensing for hydrologic systems: Water Resources Research, v. 42, W12202, accessed June 24, 2011 at doi:10.1029/2006WR005326.

Shaffer, J.A., Beirne, M., Ritchie, T., Paradis, R., Barry, D., and Crain, P., 2009, Fish habitat use response to anthropogenic induced changes of physical processes in the Elwha estuary, Washington, USA: Hydrobiologia, v. 636, p. 179-190.

Shafroth, P.B., Fuentes, T.L., Pritekel, C., Beirne, M.M., and Beauchamp, V.B., 2011, Vegetation of the Elwha River estuary, chap. 8 *of* Duda, J.J., Warrick, J.A., and Magirl, C.S., eds., Coastal habitats of the Elwha River, Washington—Biological and physical patterns and processes prior to dam removal: U.S. Geological Survey Scientific Investigations Report 2011-5120, p. 225-248.

Tyler, S.W., Selker, J.S., Hausner, M.B., Hatch, C.E., Torgersen, T., Thodal, C.E., and Schladow, S.G., 2009, Environmental temperature sensing using Raman spectra DTS fiber-optic methods: Water Resources Research, v. 45, W00D23, doi:10.1029/2008WR007052.

Turner Designs, Inc., 2004, SCUFA Self-Contained Underwater Fluorescence Apparatus user's manual: Sunnyvale, Calif., Turner Designs, Inc., 43 p., accessed June 24, 2011, at http://www.turnerdesigns.com/t2/doc/manuals/scufa_manual.pdf.

Turnipseed, D.P., and Sauer, V.B., 2010, Discharge measurements at gaging stations: U.S. Geological Survey Techniques and Methods, book 3, chap. A8, 87 p.

U.S. Geological Survey, 2007, Annual water data reports: U.S. Geological Survey Annual Water Data Reports, accessed June 24, 2011 at http://wdr.water.usgs.gov/.

Valett, H.M., Crenshaw, C.L., and Wagner, P.F., 2002, Stream nutrient uptake, forest succession, and biogeochemical theory: Ecology, v. 83, p. 2888-2901.

Valett, H.M., Morrice, J.A., Dahm, C.N., and Campana, M.E., 1996, Parent lithology, surface-groundwater exchange, and nitrate retention in headwater streams: Limnology & Oceanography, v. 41, p. 333-345.

Wagner, B.J., and Harvey, J.W., 1997, Experimental design for estimating parameters of rate-limited mass transfer—Analysis of stream tracer studies: Water Resources Research, v. 33, p. 1731-1741.

Warrick, J.A., Draut, A.E., McHenry, M.L., Miller, I.M., Magirl, C.S., Beirne, M.M., Stevens, A.W., and Logan, J.B., 2011a, Geomorphology of the Elwha River and its delta, chap. 3 *of* Duda, J.J., Warrick, J.A., and Magirl, C.S., eds., Coastal habitats of the Elwha River, Washington—Biological and physical patterns and processes prior to dam removal: U.S. Geological Survey Scientific Investigations Report 2011-5120, p. 47-74.

Warrick, J.A., George, D.A., Gelfenbaum, G., Kaminsky, G., and Beirne, M., 2009, Beach morphology and change along the mixed grain-size delta of the Elwha River, Washington: Geomorphology, v. 111, p. 136-148. doi:10.1016/j.geomorph.2009.04.012.

Warrick, J.A., and Stevens, A.W., 2011, A buoyant plume adjacent to a headland—Observations of the Elwha River plume: Continental Shelf Research, v. 31, p. 85-97, doi:10.1016/j.csr.2010.11.007.

Warrick, J.A., Stevens, A.W., Miller, I.M., and Gelfenbaum, G., 2011b, Coastal processes of the Elwha River delta, chap. 5 *of* Duda, J.J., Warrick, J.A., and Magirl, C.S., eds., Coastal habitats of the Elwha River, Washington—Biological and physical patterns and processes prior to dam removal: U.S. Geological Survey Scientific Investigations Report 2011-5120, p. 111-130.

Wunderlich, R.C., Winter, B.D., and Meyer, J.H., 1994, Restoration of the Elwha River ecosystem: Fisheries, v. 19, no. 8, p. 11-19.

Yorke, T.H., and Oberg, K.A., 2002, Measuring river velocity and discharge with acoustic Doppler profilers: Flow Measurement and Instrumentation, v. 13, p. 191-195.